Cretaceous Research (2001) **22,** 795–827
doi:10.1006/cres.2001.0291, available online at http://www.idealibrary.com on IDEAL®

Maastrichtian to Paleocene depositional environment of the Dakhla Formation, Western Desert, Egypt: sedimentology, mineralogy, and integrated micro- and macrofossil biostratigraphies

***A. A. Tantawy, †G. Keller[1], ‡T. Adatte, §W. Stinnesbeck, ¶A. Kassab and §P. Schulte**

**Department of Geology, Faculty of Science, South Valley University, Aswan, 81528 Egypt*
†*Department of Geosciences, Princeton University, Princeton, NJ 08544, USA*
‡*Geological Institute, University of Neuchâtel, Neuchâtel CH-2007, Switzerland*
§*Geological Institute, University of Karlsruhe, Karlsruhe D-76128, Germany*
¶*Geology Department, Faculty of Science, Assiut University, Assiut, 71516 Egypt*

Revised manuscript accepted 19 October 2001

Integrated sedimentology, mineralogy, geochemistry, and microfossil and macrofossil biostratigraphies of the Maastrichtian–early Paleocene Dakhla Formation of the Western Desert, Egypt, provide improved age resolution, information on the cyclic nature of sediment deposition, and the reconstruction of depositional environments. Age control based on integrated biostratigraphies of planktic foraminifera, calcareous nannofossils and macrofossils yields the following ages for stratigraphic and lithologic sequences. The contact between the Duwi and Dakhla formations marks the Campanian/Maastrichtian boundary (zone CF8a/b boundary) and is dated at about 71 Ma. The age of the Dakhla Formation is estimated to span from 71 Ma at the base to about 63 Ma at the top (zones CF8a–Plc). The Cretaceous/Tertiary (K/T) boundary is within the upper unit of the Kharga Shale Member and marked by a hiatus that spans from 64.5 Ma in the lower Paleocene (base Plc) to at least 65.5 Ma (base CF2, base *M. prinsii* zones) in the upper Maastrichtian at Gebel Gifata, the type locality of the Dakhla Formation. As a result, the Bir Abu Minqar horizon, deposited between about 64.2 and 64.5 Ma (Plc(l) zone), directly overlies the K/T boundary hiatus. Major hiatuses also span the late Maastrichtian–early Paleocene in sections to the northwest (*c.* 61.2–65.5 Ma at North El Qasr, *c.* 61.2–69 Ma at Bir Abu Minqar and *c.* 61.2–65.5 Ma at Farafra), and reflect increased tectonic activity.

During the Maastrichtian–early Paleocene a shallow sea covered the Western Desert of Egypt and the clastic sediment source was derived primarily from tectonic activity of the Gilf El Kebir spur to the southwest of Dakhla and the Bahariya arch. Uplift in the region resulted in major hiatuses in the late Maastrichtian–early Paleocene with increased erosion to the southwest. The area was located near the palaeoequator and experienced warm, wet, tropical to subtropical conditions characterized by low seasonality contrasts and predominantly chemical weathering (high kaolinite and smectite). A change towards perennially more humid conditions with enhanced runoff (increased kaolinite) occurred towards the end of the Maastrichtian and in the early Paleocene with shallow seas fringed by *Nypa* palm mangroves. Sediment deposition was predominantly cyclic, consisting of alternating sandstone/shale cycles with unfossiliferous shales deposited during sea-level highstands in inner neritic to lagoonal environments characterized by euryhaline, dysaerobic or low oxygen conditions. Fossiliferous calcareous sandstone layers were deposited in well-oxygenated shallow waters during sea-level lowstand periods.

KEY WORDS: Maastrichtian; K/T; mineralogy; sedimentology; biostratigraphy; Western Desert; Egypt.

1. Introduction

Upper Cretaceous marine sediments of the Western Desert of Egypt have been of intense economic interest due to the phosphate-rich deposits of the Duwi Formation that form part of an extensive Middle East–North Africa phosphate province. The Dakhla Formation (introduced by Said, 1961) marks the Maastrichtian–lower Paleocene sequence exposed at Gebel Gifata in the Dakhla Oasis and spans

[1]Corresponding author: gkeller@princeton.edu

0195–6671/01/060795+33 $35.00/0

Figure 1. Photograph of Gebel Gifata showing Campanian through Maastrichtian shales and calcareous sandstones topped by Paleocene limestones.

the interval between the Duwi Formation of late Campanian age and the overlying Tarawan Formation of late Paleocene age. The Dakhla Formation is of particular interest because of its rhythmic deposition of shales and glauconite-rich facies. Consequently, numerous studies have been published on the geology, stratigraphy, and sedimentology of the Maastrichtian–Paleocene marine sediments exposed in the Dakhla-Farafra District of the Western Desert (e.g. Said; 1961, 1962; Hermina *et al.*, 1961; Abbas & Habib, 1969; Awad & Abed, 1969; Issawi, 1972; El-Dawoody & Zidan, 1976; Omara *et al.*, 1976, 1977; Garrison *et al.*, 1979; Barthel & Hermann-Degen, 1981; Mansour *et al.*, 1982; Faris, 1984; Hendriks *et al.*, 1987; Luger & Schrank, 1987; Luger, 1988; Ganz *et al.*, 1990a, b; Glenn, 1990; Hermina, 1990; Kassab & Zakhera, 1995; Kassab *et al.*, 1995; Faris & Strougo, 1998).

One of the major problems encountered by all investigators was the poor age control of Upper Cretaceous stratigraphic sequences in the Western Desert as a result of a poor fossil record. Exceptions are the outcrops of the Farafra Oasis, which are rich in microfossils (Hottinger, 1960; Said & Kerdany, 1961; Youssef & Abdel Aziz, 1971; Samir, 1994, 1995; Abdel-Kireem & Samir, 1995; Tantawy, 1998), and the Cenomanian deposits of the Bahariya Formation to the north (Slaughter & Thurmond, 1974; Dominik, 1985; Allam, 1986; Werner, 1989; Smith *et al.*, 2001). Consequently, age control in most studies of the Dakhla Formation was limited to assigning an undifferentiated Maastrichtian age, and correlation of sequences was frequently based on the lithology of formations (e.g., upper Campanian Duwi Formation, Maastrichtian Dakhla Formation, Paleocene Tarawan Formation). This provided little or no information on the timing of events within these formations, or the correlation of these events from one region to another. This report concentrates on the Dakhla Formation, which is exposed over several hundreds of kilometers in an east–west trending belt in the Western Desert of Egypt where it forms the slope of horizontally stratified table mountains that are capped by Paleocene limestone beds of the Tarawan Formation (Figure 1). We examined five outcrop localities between Dakhla and Farafra Oasis (Figure 2). The major objectives of this study have been to: (1) determine the lithological characteristics of a number of key outcrops in the southwestern Desert; (2) determine the age and depositional environment of the Maastrichtian Dakhla Formation based on integrated microfossil (planktic foraminifera and nannofossils) and macrofossil

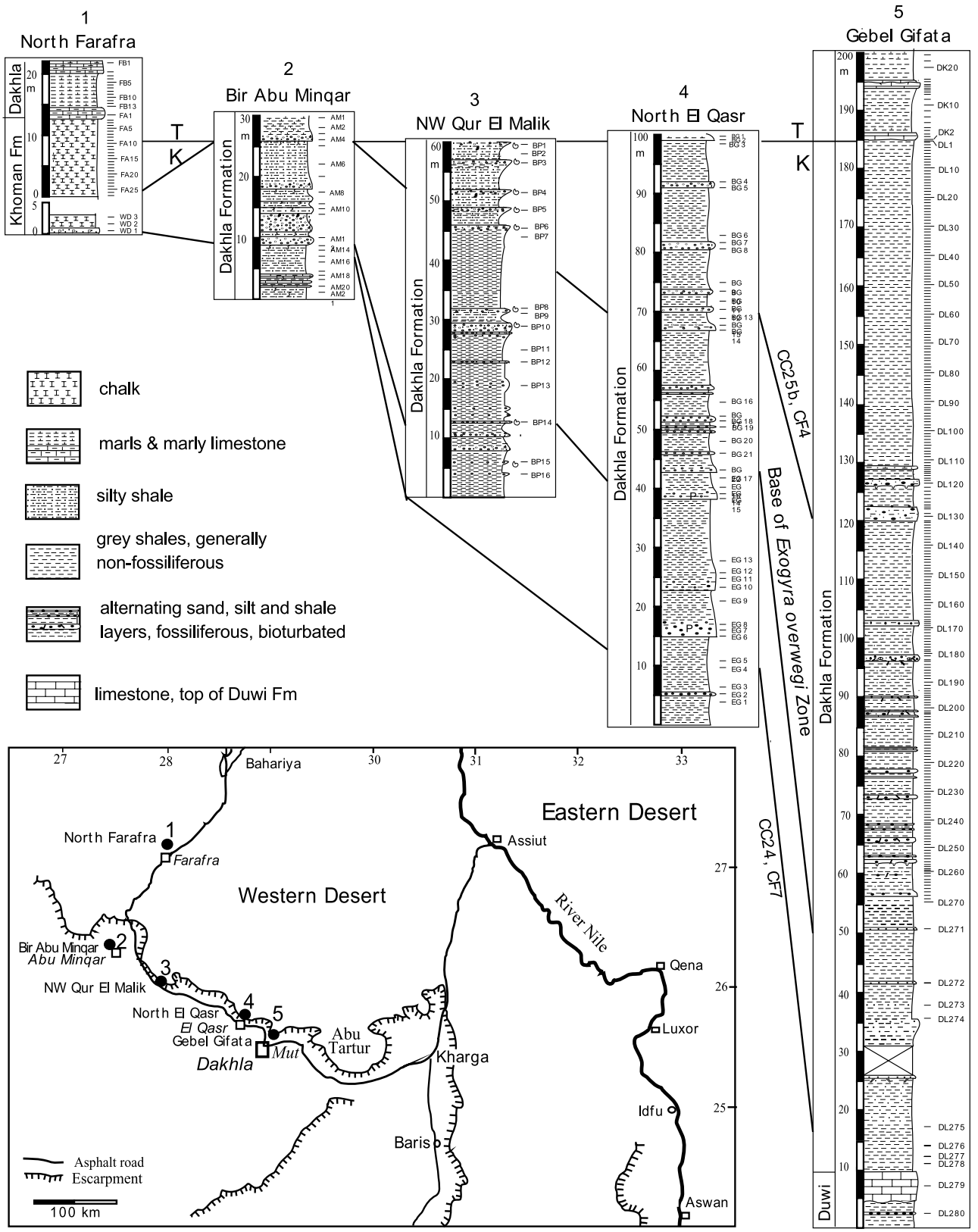

Figure 2. Location map of sections analyzed and their lithological columns correlated based on the K/T boundary disconformity, planktic foraminiferal zones CF4 and CF7, calcareous nannofossil zones CC25b and CC24, and the base of the *Exogyra overwegi* Zone. Note that in Northwest Qur El Malik no microfossils were recovered, although macrofossils are present.

biostratigraphies; (3) geochemically evaluate the shale-sandstone cycles and their depositional environment; (4) reconstruct the regional environmental history.

2. Location and sampling

The Gebel Gifata section is located in the Western Desert approximately 15 km north of Mut in the Dakhla Oasis (Figure 2). Gebel Gifata is the type locality of the Dakhla Formation and is part of a mountain scarp that limits the topographic depression of the Dakhla Oasis towards the north and east to the plateau of the Paleocene limestone of the Tarawan Formation (Figure 1). The section was measured and sampled on the slope where a 195-m-thick sequence spans the uppermost Duwi and Dakhla formations, and the strata dip (<10°) towards the south (towards the oasis). The basal part of the section (*c.* 25m) is not exposed at the main outcrop at Gebel Gifata and was therefore measured at the northwestern border of the El Owaina village, about 10 km north of Mut. Two hundred and eighty samples were collected at approximately 50 cm intervals from the upper Campanian and Maastrichtian, and 20 were taken from the lower Paleocene interval.

The North El Qasr section is located 30 km northwest of Mut and approximately 5 km north of the El Qasr Village (Figure 2). Thirty-nine samples were collected from a 100-m-thick interbedded shale, silt, and sandstone sequence spanning the Maastrichtian–lower Paleocene. About 120 km northwest of El Qasr village is the Qur El Malik section where we measured a 60-m-thick lower Maastrichtian shale and sandstone sequence and collected 16 samples. About 260 km northwest of Mut at the bend of the Dakhla-Farafra road is the Bir Abu Minqar section located at the foot of the scarp immediately north of the village of Abu Minqar. Twenty-one samples were collected from a 30-m-thick shale and sandstone sequence that is rich in macrofossils and spans the Maastrichtian to lower Paleocene. The Farafra section is located about 15 km north of Qasr El Farafra (350 km northwest of Mut) at the North Gunna locality that is marked by a group of three isolated conical hills. Forty samples were collected from a 22-m-thick chalk sequence spanning the Khoman, Dakhla and Tarawan formations. The basal part of the section was sampled in the White Desert, about 25 km to the north. Sediments at this locality consist of a phosphatic sandstone layer that underlies a thick chalk sequence.

3. Methods

All sections were measured and examined for lithological changes, macrofossils, trace fossils, bioturbation, erosion surfaces and hardgrounds. Samples for microfossils were collected at 20–50-cm intervals as indicated in the figures, and macrofossils were collected wherever present.

For foraminiferal studies, samples were processed following the standard method of Keller *et al.* (1995). Calcareous nannofossils were processed by standard smear slide preparation from raw sediment samples as described by Perch-Nielsen (1981a, b, 1985). Index species are illustrated in Figures 19 and 20.

Phosphate (P) geochemistry (SEDEX method) was conducted for selected intervals with the sequential extraction method (Ruttenberg, 1992; Ruttenberg & Berner, 1993; Anderson & Delaney, 2000). This method chemically isolates P from four P-bearing phases, depending on dissolution characteristics. The four extracted phases in their determined order are adsorbed and ironbound P, authigenic P, detrital P, and organic P. For steps 2–4, phosphate solutions were analyzed spectrophotometrically with the standard ascorbic acid molybdate blue technique. Sample absorbance and P concentration calculations were performed using an Elmer Perkin X200 scanning spectrophotometer. Solutions from the first step and the Fe and Mn contents were analyzed by ICP-MS.

Whole rock and clay mineral compositions were analysed at the Geological Institute of the University of Neuchâtel, Switzerland using a SCINTAG XRD 2000 Diffractometer. Whole rock compositions were determined by XRD based on methods described by Kübler (1983). Clay mineral analyses followed the analytical method of Kübler (1987) described in Adatte *et al.* (1996). We present here data from the <2 μm size fraction. Clay minerals are given in relative percent abundance.

4. Lithology and depositional environment

Among the five sections examined, the type section of the Dakhla Formation at Gebel Gifata provides the most expanded sequence spanning the late Campanian to the early Paleocene. All other sections can be referenced to and correlated with Gebel Gifata. The Dakhla Formation at the type section spans about 200 m and is divided into Mawhoob Shale, Beris Mudstone and Lower and Upper Kharga Shale members (Figure 3).

At the base of the Gebel Gifata section the upper part of the upper Campanian Duwi Formation is exposed. The sediments consist of alternating shale and phosphatic beds capped by a 5-m-thick white micritic and phosphatic limestone with *Chondrites* burrows in the basal 10 cm (Figure 3). This limestone bed was referred to by Abbas & Habib (1969) as

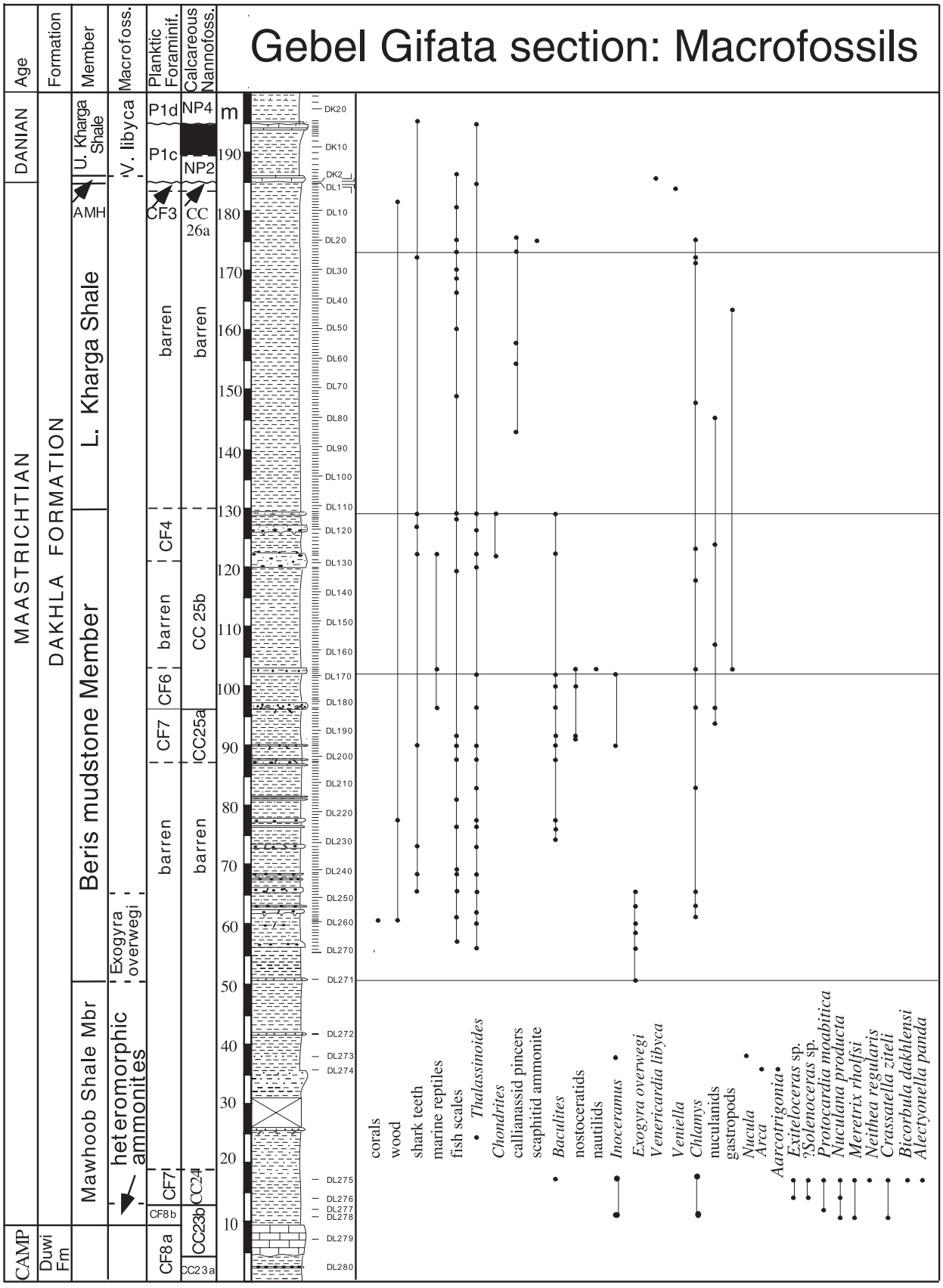

Figure 3. Lithological column, sample intervals, integrated microfossil and macrofossil biostratigraphies, and macrofossil ranges at the Gebel Gifata section for the Late Campanian–Early Paleocene.

'*Isocardia chargensis* limestone' and subsequently by Barthel & Herrmann-Degen (1981) as Qur-el-Malik Member of the Dakhla Formation.

The Dakhla Formation is of Maastrichtian–early Paleocene age and begins at the top of this phosphatic limestone. In the lower 40 m (Mawhoob Shale Member) sediments generally consist of dark grey siltstones and shales. In the overlying 80 m (Beris Mudstone Member), siltstones and shales are intercalated with light grey to brown sandstones. Above the Beris Mudstone are about 55 m of monotonous shales (Lower Kharga Shale) of late Maastrichtian age, followed by 15 m of shale containing two prominent units consisting of silty limestone and glauconitic sandstone that mark the early Paleocene (Upper Kharga Shale) of the Dakhla Formation (Figures 2, 3).

At least 23 calcareous sandstone layers are present in the lower 130 m of the Dakhla Formation (Mawhoob Shale Member and Beris Mudstone Member; Figure 3). These calcareous sandstone beds range from a few cm to 1.5 m thick and contain a heterogenous variety of phosphatic particles, fish debris, rare vertebrate remains and microfossils (Figures 3, 4). The lower surfaces of the calcareous sandstone layers are usually erosive and associated with abundant *Thalassinoides* burrowing networks that extend from the sharp lithological contact down into the underlying dark-coloured siltstones and shales. The upper contact of the calcareous sandstone layers is usually gradual and formed by light grey siltstones that are mottled and generally rich in invertebrate shells (bivalves, gastropods, occasional cephalopods). Above the calcareous sandstone layers, oxygen and energy levels tend to be more reduced, as indicated by light-coloured siltstones with occasional *Chondrites* feeding structures. In the 55-m-thick Lower Kharga Shale, these sediments grade into monotonous dark grey siltstones and shales that are fissile, organic-rich, and frequently laminated, indicating dysaerobic conditions (Figure 5). Both body and trace fossils are rare in these dark siltstones and shales, except for fish scales, callianassid pincers, small pectinid bivales and occasional small nuculanid bivalves (Figure 3).

The dark shales, siltstones and interbedded calcareous sandstone layers change laterally towards the west with increasing sand and decreasing shale contents. In the sections of Northwest Qur el Malik and Bir Abu Minqar, the sediments are composed primarily of silty shales and thick calcareous sandstone beds that are rich in *Exogyra overwegi* and sphenodiscid ammonites (Ammonite Hill Member of Barthel & Herrmann-Degen, 1981) of early–early late Maastrichtian age (Figures 2, 3). Towards Farafra in the northwest, the Lower Kharga Shales abruptly change to thick deposits of chalk and chalky limestone of the Khoman Formation.

5. Cretaceous/Tertiary contact

A major K/T hiatus is present in all of the sections examined. At Gebel Gifata, the K/T contact was placed at the base of a 1-m-thick tan-coloured calcareous siltstone and sandy limestone sequence that is widespread in the region and marks the base of the Abu Minqar horizon (Figure 6; Abbas & Habib, 1969; Barthel & Hermann-Degen, 1981; Mansour *et al*, 1982). The unit is easily recognized along the slope of Gebel Gifata as it disconformably overlies the monotonous 55-m-thick sequence of dark-grey shale of the Lower Kharga Shale Member at approximately 185 m above the base of the section. The K/T disconformity is prominently marked by an undulating erosional surface between the dark grey shale and overlying tan-coloured calcareous sandstone that contains mudclasts, macrofossils (bivalves), and impoverished late Maastrichtian planktic foraminiferal and calcareous nannofossil assemblages (Figure 7). Thin sections indicate uneven dissolution of foraminiferal shells, transport, winnowing and accumulations in depressions. From the lower contact of this layer, diagonal to vertical unbranched burrows extend 40 cm into the underlying dark grey silty shales that are also fossiliferous.

Above the K/T disconformity a sedimentologically complex sequence marks the Bir Abu Minqar horizon (Figures 6, 7) that consists of three amalgamated limestone-sandstone beds with undulose and erosive lower contacts and intensive burrowing into the underlying sediments. The lowermost layer consists of tan-coloured calcareous sandstone that contains abundant macrofossils (e.g., *Venericardia libyca*), benthic and planktic foraminifera (Figure 7). Above this layer is a 40-cm-thick yellow to tan-coloured calcareous siltstone with an undulose and erosive upper contact (Figure 6). The calcareous siltstone layer is homogenous, contains calcareous nannofossils, small benthic foraminifera and planktic foraminifera, including the first diverse early Danian assemblage indicative of zone P1c (Figure 7). The unit is intensively burrowed from above. These burrows are filled with the yellow sandy limestone that forms the 10-cm-thick layer at the top of the unit. A 30-cm-thick glauconitic calcareous sandstone layer overlies the erosive contact. The basal 10 cm are microconglomeratic and contain rounded clasts of yellow marly limestone, shale, sandstone, glauconite grains, Fe-rich lithoclasts and multi-compound phosphatic particles,

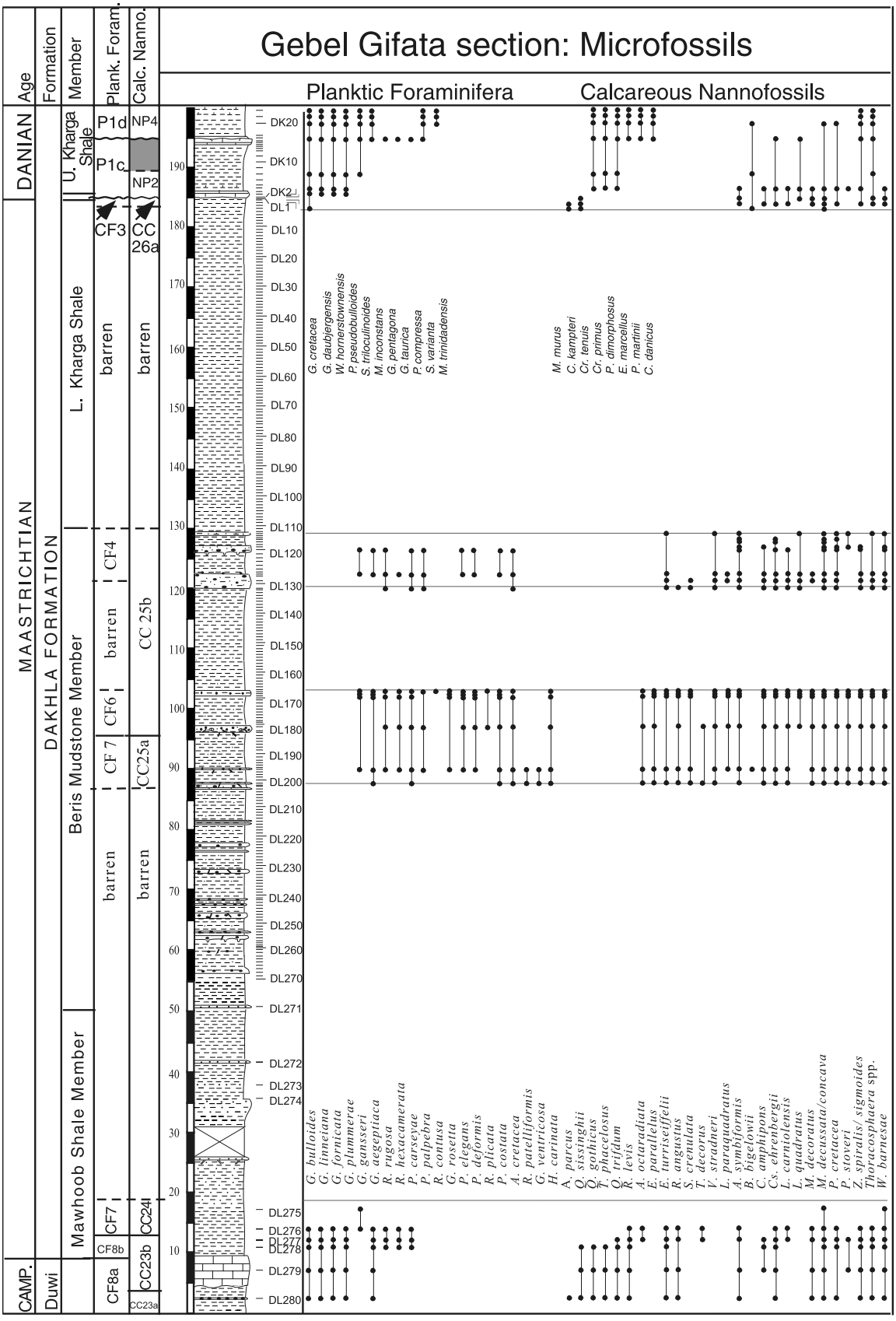

Figure 4. Lithological column, sample intervals, integrated microfossil biostratigraphies, and species ranges of calcareous nannofossils and planktic foraminifera at Gebel Gifata for the Late Campanian–Early Paleocene.

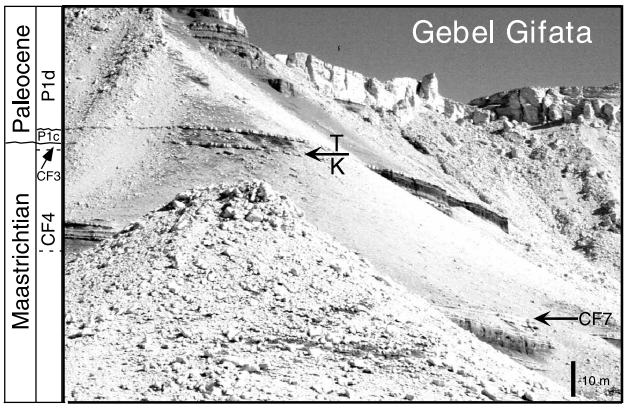

Figure 5. Photograph of the upper Maastrichtian Beris Mudstone Member (planktic foraminiferal zone CF4 and calcareous nannofossil zone CC25b) and the lower Paleocene Upper Kharga Shale Member (zones Plc and NP2) at Gebel Gifata. The K/T boundary and lower Paleocene are well marked by two resistant calcareous sandstone layers.

shark teeth and interior moulds of gastropods (Figure 3). Up-section, the light-grey phosphatic microconglomerate grades into grey calcareous sandstone and dark-grey siltstone. The overlying 8 m of sediment consist of dark grey fissile shale (Figure 6).

A second metre-thick sequence of limestones, glauconitic sand and phosphatic particles is present about 9 m above the K/T boundary at Gebel Gifata (Figure 7). This unit consists of two layers of yellow sandy limestones, each approximately 50 cm thick, that contain shell hash of small recrystallized venericardid bivalves, abundant benthic and rare planktic foraminifera. Rounded clasts of yellow marly limestone up to 10 cm in diameter are also present in the lower 10 cm of the limestone layer and indicate intensive erosion from a nearby shallow-water area. The basal layer is a tan-coloured micritic limestone with an undulose and erosive lower contact. Burrows extend from this contact into the underlying dark grey shales. The upper limestone layer is phosphatic and glauconitic at the base. The sand-sized, rounded, green glauconite pellets and Fe-rich brown-grey grains reach 3 mm in diameter. Small siltstone clasts are also present and benthic foraminifera are abundant. The glauconitic sand fills pockets and burrows that extend into the lower layer. Above this interval, the glauconitic sand grades into a tan-coloured bioclastic packstone rich in recrystallized venericardid bivalves and abundant benthic and rare planktic foraminifera and calcareous nannofossils (Figures 3, 7). Karst-like fractures filled with glauconite extend from the top of this layer almost to the base and suggest subaerial exposure and erosion prior to deposition of the overlying 30-cm-thick glauconite in a marine environment. This glauconite layer contains well-rounded sand-sized glauconite pellets and phosphatic grains up to 5 mm in diameter, rare bivalves, gastropods, and abundant benthic and planktic foraminifera. Above this interval, the glauconite grades into a 10-m-thick grey shale.

At Bir Abu Minqar, the K/T contact is at a disconformity between shale and the overlying glauconitic and phosphatic sandstone. At North Farafra, the K/T contact occurs within the chalk of the Khoman Formation about 3 m below the basal limestone of the Dakhla Formation as discussed below. Biostratigraphy indicates that the interval represented by the Khoman chalk is missing at Bir Abu Minqar, probably because of the disconformity (Figure 1). The absence of limestone deposition further to the south was a result of a shallowing of the sea during the late Maastrichtian (see Li *et al.*, 1999, 2000), and terrigenous influx that prevented chalk deposition. A 2-m-thick limestone bed separates the Khoman Formation from the overlying 10-m marl sequence of the Dakhla Formation at North Farafra.

6. Integrated macro- and microfossil stratigraphies

Planktic foraminifera and calcareous nannofossils are generally present in glauconite-rich intervals in all sections examined, but rare or absent in shale lithologies. At the Farafra section, foraminifera are present throughout the section, but show strong dissolution effects. Most Maastrichtian zones could be identified, although the positions of their upper and lower boundaries are uncertain because barren intervals separate the short intervals with well-preserved and diverse assemblages. Nevertheless, a late Campanian through Danian biostratigraphic sequence could be determined based on both planktic foraminifera and calcareous nannofossils. The zonal schemes used in this study are briefly outlined below and correlated with commonly used zonal schemes (Figure 8).

The standard planktic foraminiferal zonal scheme divides the Maastrichtian into three zones (*Abathomphalus mayaroensis*, *Gansserina gansseri* and *Globotruncana aegyptiaca*; Figure 8). In this study we use the new zonal scheme by Li & Keller (1998a, b) who subdivided the Maastrichtian into nine zones labelled CF1–CF8a and b (CF for Cretaceous Foraminifera) that provide higher resolution age control. This new zonation was developed based on high resolution quantitative planktic foraminiferal analyses of DSDP Site 525 and sections in Tunisia. The biozonation for the K/T transition and lower Danian is from Keller *et al.* (1995). Age estimates for Late

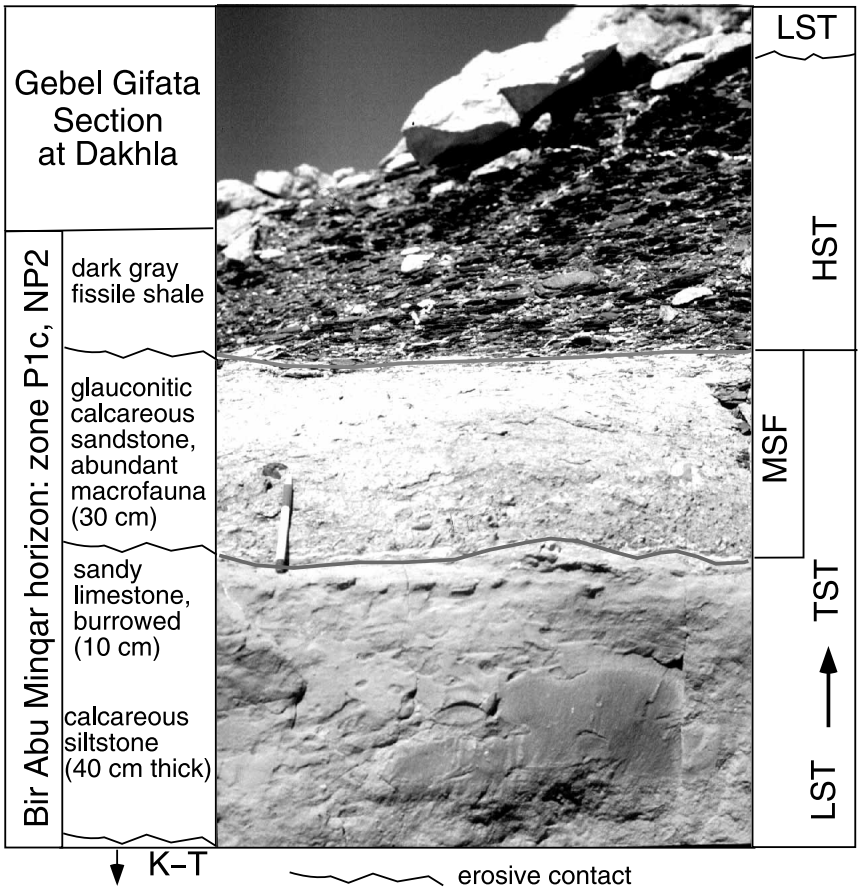

Figure 6. Photograph of the Bir Abu Minqar horizon at Gebel Gifata showing repeated erosion between calcareous sandstone, siltstone and glauconitic sandstone. MSF, maximum flooding surface; HST, sea-level highstand; LST, sea-level lowstand; TST, transgressive system track.

Cretaceous zones are based on foraminiferal datum events of DSDP Site 525 tied to the palaeomagnetic stratigraphy of the same core. Age extrapolation for the Tunisian sections is based on biostratigraphic correlation and event stratigraphy, including sea-level changes and stable isotope stratigraphy (Li *et al.*, 1999, 2000). These datum events and biozones are broadly valid for the eastern Tethys region, including Egypt. In the Western Desert of Egypt, nine planktic foraminiferal zones could be recognized spanning the time interval from the late Campanian to the late Paleocene.

Calcareous nannofossil zonation for the Danian is based on low–middle latitude nannofossil zonal schemes by Sissingh (1977) and Roth (1978) for the Maastrichtian, and Martini (1971) for the Paleocene. These zonal schemes were subsequently subdivided by Perch-Nielsen (1979, 1981a, b, 1983), Romein (1979), Okada & Bukry (1980) and Doeven (1983) (Figure 8). Seven calcareous nannofossil zones could be identified in this study.

Macrofossils are generally scarce in Maastrichtian–Paleocene sections in Egypt, as well as worldwide, and many of the species present are long-ranging and, therefore, provide limited age control. Kassab *et al.* (1995) published a revised macrofossil biozonation for the Western Desert, and although some of the proposed zones are ecologically restricted to the area, others provide excellent marker horizons over wide geographic regions. For example, the *Exogyra overwegi* Zone is approximately equivalent to the lower part of planktic foraminiferal zone CF7 and lower part of calcareous nannofossil zone CC25a. *Venericardia libyca* is characteristic of the Danian, and heteromorphic ammonites (*Solenoceras*, *Exiteloceras*, and ?*Bostrycoceras*) occur regionally at the base of the Dakhla Formation, coincident with zones CF8b and CC23b (Figure 3).

6.1. *Upper Campanian*

The oldest fossiliferous sediments were encountered near the base of the Gebel Gifata section in the

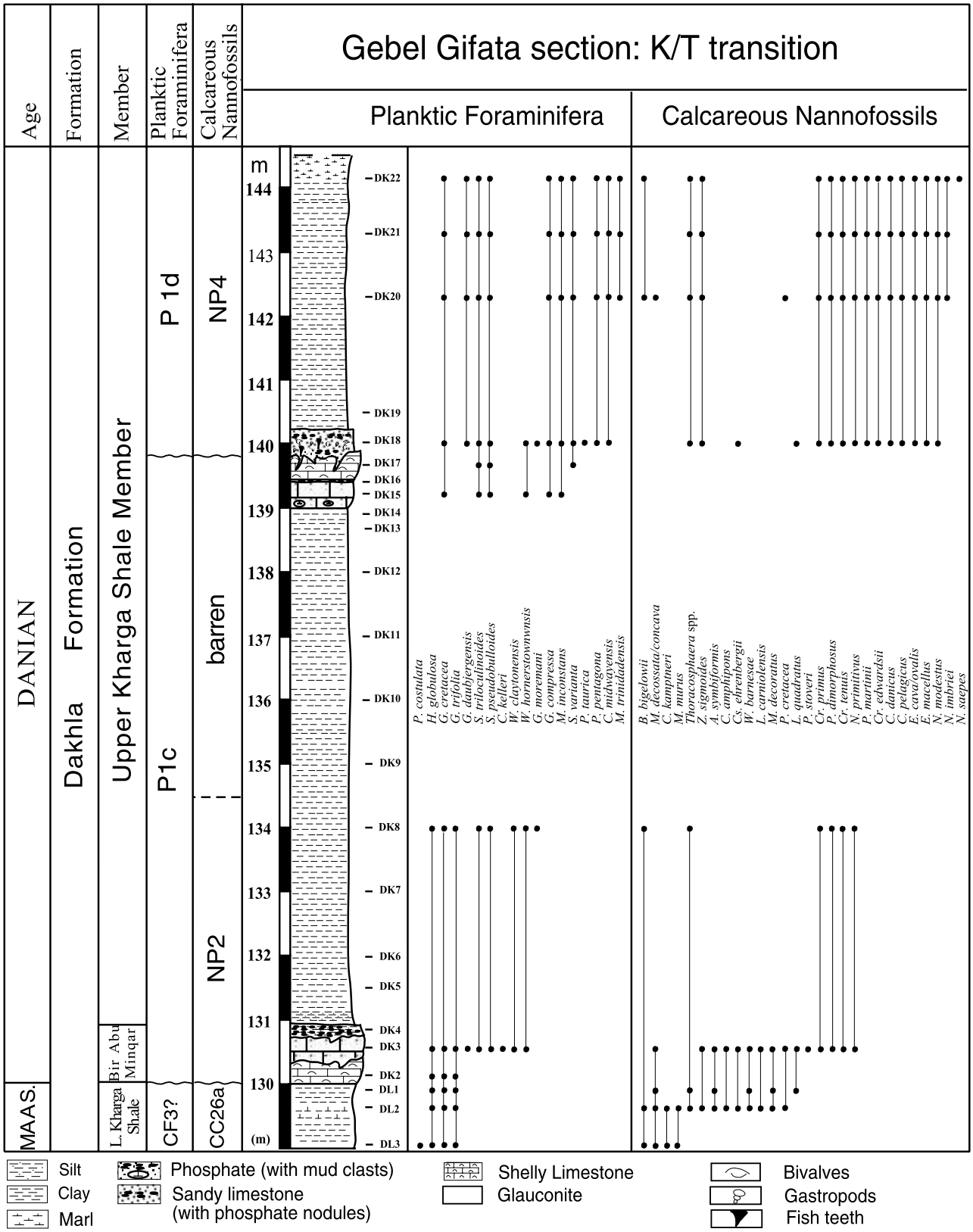

Figure 7. Details of lithology, sample intervals, biostratigraphies and species occurrences of planktic foraminifera and calcareous nannofossils across the Cretaceous/Tertiary boundary at the Gebel Gifata section. The two resistant calcareous sandstone and siltstone layers form prominent stratigraphic horizons in the outcrop photograph, Figure 5.

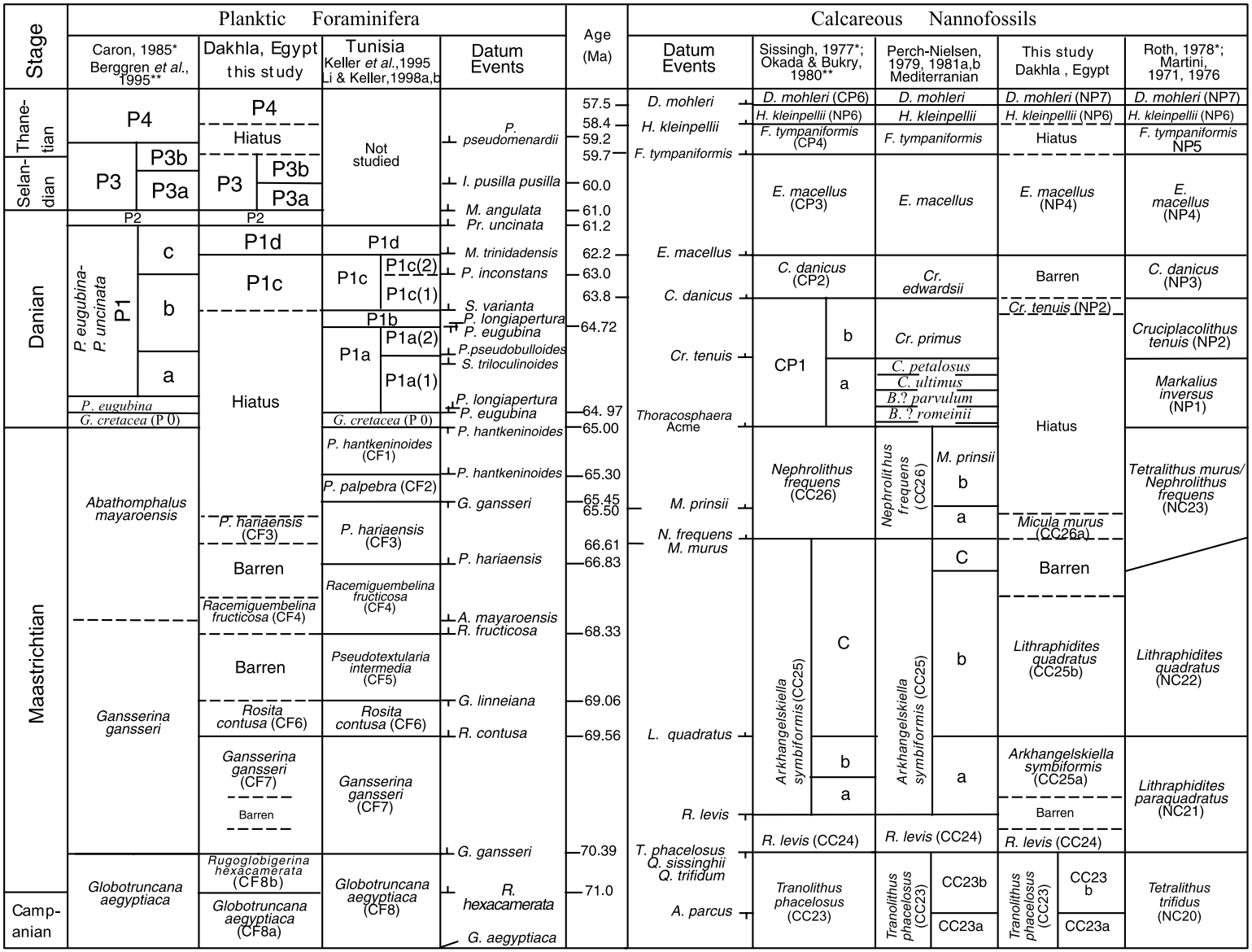

Figure 8. Summary of commonly used planktic foraminiferal and calcareous nannofossil zonal schemes, age estimates, and their recognition in the Western Desert of Egypt. The datum events for Maastrichtian planktic foraminiferal zones are based on the palaeomagnetic record, the foraminiferal ranges of DSDP Site 525A, and biostratigraphic correlations to sections in Tunisia (Li & Keller, 1998a, b).

phosphatic sandstone and micritic limestone that mark the top of the Duwi Formation. Planktic foraminiferal assemblages in this interval are characterized by *Globotruncana aegyptiaca*, *G. bulloides*, *G. linneiana*, *G. fornicata* and *G. plummerae* and indicate a latest Campanian age, or zone CF8a (Figure 4). The lowermost 3 m of the overlying Dakhla Formation contain well-preserved, abundant and diverse assemblages including common rugoglobigerinids, such as *Rugoglobigerina rugosa* and *R. hexacamerata*, along with *G. bulloides*, *G. fornicata*, *G. linneiana*, *G. plummerae* and *Planoglobulina carseyae*. These assemblages indicate the earliest Maastrichtian zone CF8b, as suggested by the absence of *Gansserina gansseri* and presence of *R. hexacamerata*. The calcareous nannofossil assemblages are represented by *Aspidolithus parcus*, *Quadrum gothicus*, *Q. sissinghii*, *Q. trifidum*, *Tranolithus phacelosus*, *Reinhardtites levis*, *Eiffelithus turriseiffelii*, *Rhagodiscus angustus*, *Arkhangelskiella symbiformis*, *Micula decussata* and *Prediscosphaera cretacea* (Figure 4). These assemblages indicate zone CC23, which spans the Campanian/Maastrichtian transition (Figure 8). The Campanian/Maastrichtian boundary is tentatively identified based on planktic foraminifera (zone CF8a/CF8b boundary, see below).

6.2. *Campanian/Maastrichtian boundary*

The Campanian/Maastrichtian stage boundary has not yet been formally defined because of the poor correlation between macro- and microfossil zonations. Planktic foraminiferal workers commonly place this boundary at the top of the *Globotruncanita calcarata* Zone (e.g. Robaszynski *et al.*, 1983–1984; Caron, 1985; Li & Keller, 1998a, b), and calcareous nannofossil specialists have placed it within NC20 (Bralower *et al.*, 1995), or within CC23 (e.g., Sissingh, 1977; Perch-Nielsen, 1985). Macrofossil workers place this boundary at the top of the *Baculites senseni* (ammonite) Zone, or the overlying *B. eliasi* Zone (e.g., Gradstein *et al.*, 1995). Stratigraphic correlations between these zonal schemes indicate that the *G. calcarata* last appearance datum (LAD) is significantly older than the macrofossil zone that defines the Campanian/Maastrichtian boundary (Kennedy *et al.*, 1992). The Subcomission of Cretaceous Stratigraphy has proposed that the Campanian/Maastrichtian boundary be placed at the ammonite first appearance datum (FAD) of *Pachydiscus neubergicus* (Odin, 1996). The FAD of *P. neubergicus* has an estimated age of 71.6 ± 0.7 Ma based on linear interpolation between K/Ar ages of two bentonites (Obradovich, 1993) at the base of C32N.1n (Gradstein *et al.*, 1995). This interval corresponds to within the upper *G. aegyptiaca* Zone (CF8) and near the FA of *Rugoglobigerina hexacamerata* and *Planoglobulina carseyae* that subdivide CF8 into two subzones CF8a and CF8b (Li & Keller, 1998b; Li *et al.*, 1999). An alternative marker species is the first appearance of *Gansserina gansseri*, though it is significantly younger (70.39 Ma; Figure 8).

In this study, we followed Li *et al.* (1999) who used the planktic foraminifer *R. hexacamerata* FAD as a marker for the Campanian/Maastrichtian boundary. The age of this datum event is estimated at 71 Ma based on biostratigraphic correlation with the geomagnetic time scale at DSDP Site 525A (Li & Keller, 1998a). This stratigraphic interval corresponds to within the calcareous nannofossil zone CC23 and top of NC20 (see Bralower *et al.*, 1995; Li & Keller, 1998a; Figure 3). Accordingly, the Campanian/Maastrichtian boundary coincides with the lithologic boundary between the Duwi Formation and the overlying Dakhla Formation (Figure 4).

However, there are significant differences in the placement of the Campanian/Maastrichtian boundary based on macrofossils and microfossils by earlier workers. For example, a Maastrichtian age was assigned to the Duwi Formation based on the ammonite *Bostrychoceras polyplocum* (El Akkad & Dardir, 1966; Abdel Razik, 1969; Issawi *et al.*, 1978), and the bivalves *Lopha vilei*, *Ostrea* and *Alectryonia* (Hassan, 1973; El Deftar *et al.*, 1978; Issawi *et al.*, 1978). However, the same species were also used by various authors (e.g., Awad *et al.*, 1964; El Naggar, 1966; Abdel Razik, 1972) to assign a late Campanian age, suggesting that these ammonite index species and bivalves span the Campanian/Maastrichtian boundary. This was also observed by Reiss (1962) and El Naggar (1966) who correlated the ammonite *Bostrychoceras polyplocum* to the late Campanian planktic foraminiferal zone *G. calcarata*, which confirms that the Duwi Formation is of late Campanian age. More recently, Faris (1984), Schrank (1984) and Schrank & Perch-Nielsen (1985) concluded that the Dakhla shales are of Maastrichtian age and that the upper portion of the Duwi Formation may be of late Campanian–early Maastrichtian age. Based on a summary of available biostratigraphic data, Glenn (1990) concluded that the Campanian/Maastrichtian stage boundary is within the upper 10 m of the Duwi Formation at Gebel Duwi, the type locality in the Eastern Desert. Similarly, Hamama & Kassab (1990) placed the Campanian/Maastrichtian boundary near the top of the ammonite *Bostrychoceras polyplocum* Zone, coincident with the contact between the Duwi and Dakhla formations at Gebel Abu Had and Wadi Hamama. Recent studies, including ours,

thus place this stage boundary at the top of the Duwi Formation.

6.3. Lower Maastrichtian

Shales and thin silt and calcareous sandstone layers characterize the lower Maastrichtian Mawhoob Shale Member of the Dakhla Formation at Gebel Gifata (Figures 2, 3), Bir Abu Minqar (Figure 9) and North El Qasr (Figure 10). Microfossils are very rare in the lower Maastrichtian of North El Qasr and Bir Abu Minqar and indicate a zone CF7 and CC25a age (*G. gansseri* and *A. cymbiformis*; see also Hermina, 1990). The Northwest Qur El Malik section contains neither calcarous nannofossils nor foraminifera, although a relatively diverse macrofossil assemblage is present, indicating the presence of the *Exogyra overwegi* Zone (Figure 11). Ammonites are abundant in the uppermost 5 m and consist of *Libycoceras acutodorsatus* and *Brahmaites brahma*. To the north in the Farafra area, the sediments change to the chalk and chalky limestone of the Khoman Formation as a result of a deeper depositional environment beyond the reach of terrigenous influx (Figure 12). An early Maastrichtian chalk of zone CF7 and CC25a age was sampled above a prominent dark phosphate horizon in the White Desert. However, at the North Farafra section, collected in the North Gunna area, the lowermost sediment samples are of late Maastrichtian zones CF3–CF4 and CC25b age that correlate with the uppermost part of *G. gansseri* Zone of Samir (1995).

Only in the lowermost 3 m of the Dakhla Formation at Gebel Gifata was the basal Maastrichtian identified, based on microfossil assemblages that indicate planktic foraminiferal zone CF8b (FAD of *R. hexacamerata*) and nannofossil assemblages indicative of zone CC23 (Figure 4). The first *G. gansseri* (well-developed forms) appear at 14 m (DL276) and mark the base of zone CF7. This level corresponds to the base of calcareous nannofossil zone CC24 (see Figure 8). The macrofossil assemblage in this interval includes *Chlamys* (*Aequipecten*) *acuteplicatus*, *Nuculana producta*, *Inoceramus faragi*, *Alectryonella panda* and numerous impressions of heteromorphic ammonites (e.g., *Baculites*, *Exiteloceras*, *Solanoceras*; Figure 3). This ammonite fauna is known to exist on a regional scale in eastern and western Egypt (Kassab *et al.*, 1978; Kassab & Zakhira, 1995), and has also been described from the basal Dakhla Shale Member of Mut by Barthel & Herrmann-Degen (1981). Reiss *et al.* (1985) correlated this fauna to the *Bostrychoceras polyplocum* Zone of the late Campanian. In our study, these faunas are correlated with the lower parts of both the early Maastrichtian planktic foraminiferal zone CF7 and the calcareous nannofossil zone CC24 (Figure 4).

The sediments between 20 and 88 m at Gebel Gifata consist of alternating layers of dark grey siltstones and thin layers of phosphatic skeletal sands or shell hash (Figure 3). This interval is devoid of both planktic foraminifera and calcareous nannofossils. In the lower part (upper part of the Mawhoob Shale Member, between 35 and 63 m), invertebrate fossils are rare and only bivalves (e.g., *Arca*, *Arcotrigonia*, inoceramids, pectinids) were observed (DL275–271; Figure 3). However, the overlying 10–15-m-thick interval that marks the lower part of the Beris Mudstone Member (*Exogyra overwegi* Zone) is very rich in the oyster *Exogyra overwegi* (Munier-Calmas), many of which are still in life positions. *Exogyra* is a marine oyster that is widely distributed in deposits representing Late Cretaceous shelf habitats at water depths of less than 50 m (Reiss, 1984). Hence, the presence of this oyster bed indicates deposition in an inner neritic environment. In the 10 m above the *Exogyra* beds only disarticulated and fragmented specimens are present and none was found above 130 m (sample DL248, Figure 3). In the upper part of the calcareous sandstone layers of the Beris Mudstone Member *Exogyra* is absent and other megafossils are abundant, including cephalopods (*Baculites inornatus*, *Diplomoceras* sp., *Exiteloceras* sp., *Eutrephoceras* sp.), bivalves [e.g., *Chlamys* (*Aequipecten*) *acuteplicatus*, *Veniella*, *Inoceramus*, *Nuculana producta*, *Venericardia quassi*, and rare oysters], gastropods (e.g., *Turritella sexlineata*), rare solitary corals (sample DL259), shark teeth, fish bones, scales, reptile teeth (?pliosaurs), and occasionally wood and leaves (sample DL223; Figure 3). This assemblage indicates a shallow, nearshore or lagoonal environment.

Above the microfossil-barren layer at Gebel Gifata, rich planktic foraminiferal assemblages are indicative of the upper part of zone CF7, characterized by common rugoglobigerinids (*Rugoglobigerina macrocephala*, *R. rugosa*, *R. scotti*; Figure 4). Deposition of these assemblages probably occurred in a marginal marine environment with an influx of open marine species, as suggested by high foraminiferal-species richness, the presence of deeper-water (thermocline) dwelling species (globotruncanids), and the low abundance of benthic foraminifera (*c.* 10%) relative to planktic foraminifera. Calcareous nannofossil assemblages in this interval consist mainly of solution-resistant taxa, although the presence of *Lithraphidites paraquadratus* and absence of *L. quadratus* indicate the early Maastrichtian zone CC25a, correlative with planktic foraminiferal zone CF7 (Figures 4, 8). The

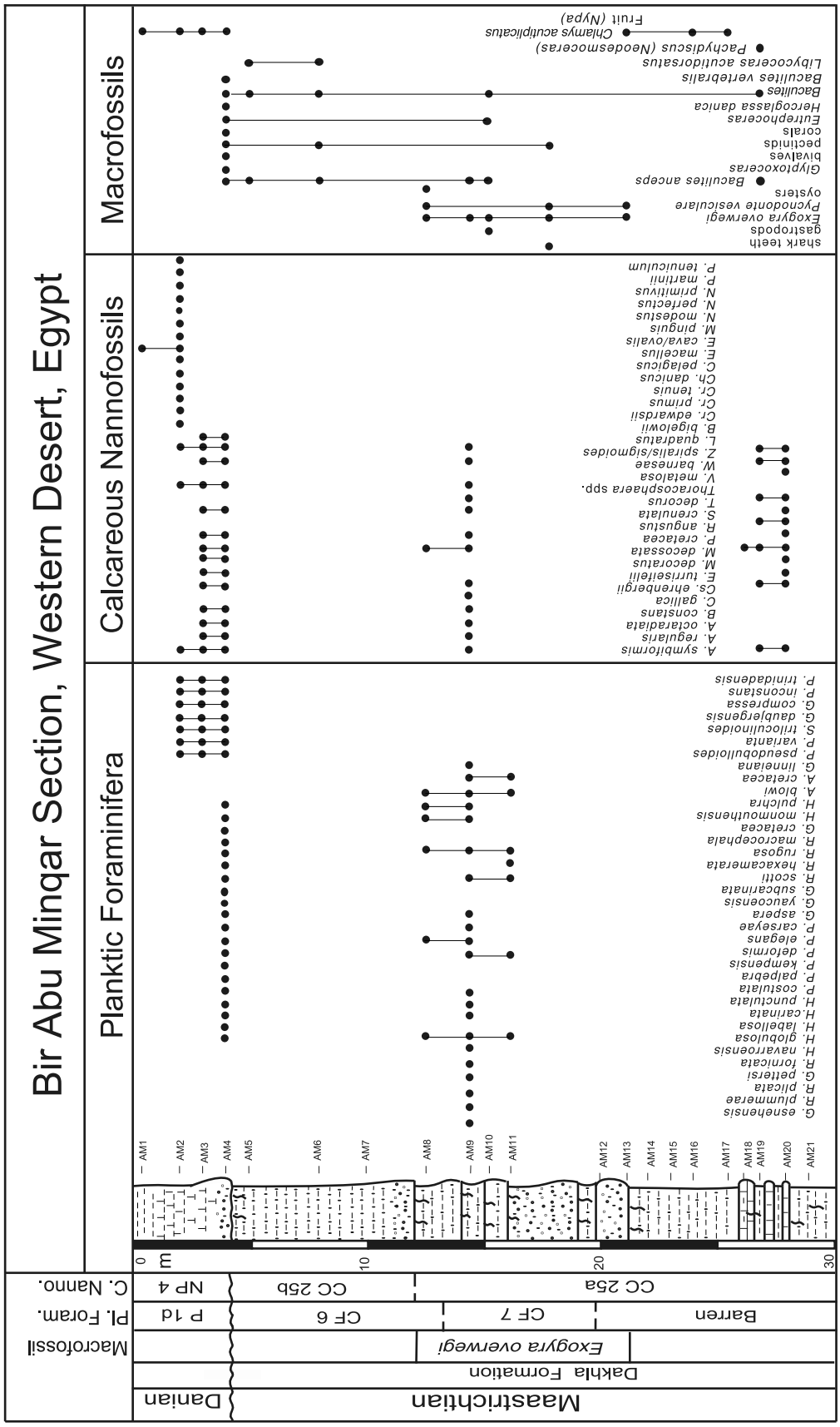

Figure 9. Lthological column, microfossil and macrofossil biozones, and species ranges of planktic foraminifera, calcareous nannofossils, and macrofossils at the Bir Abu Minqar section.

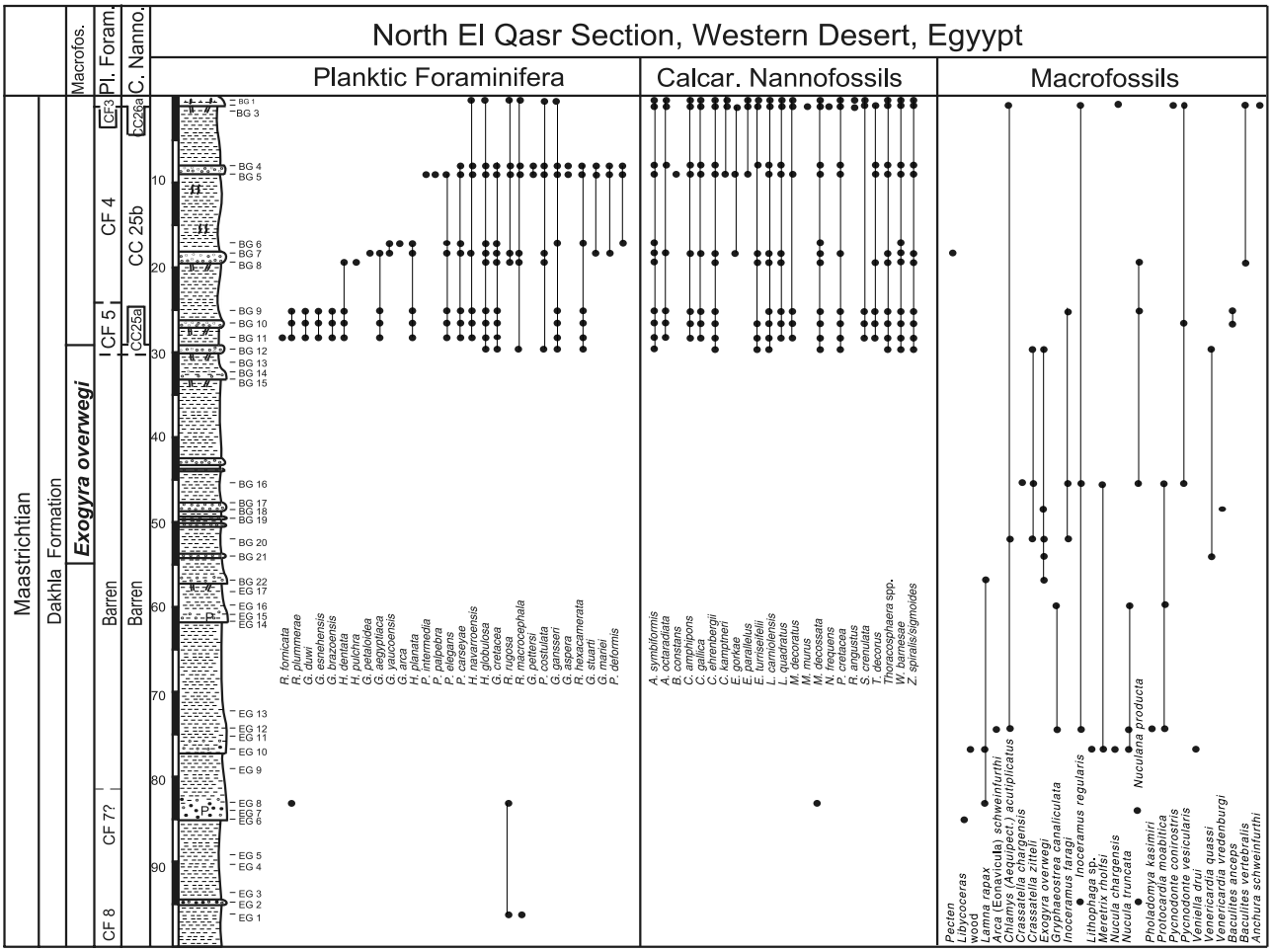

Figure 10. Lithological column, microfossil and macrofossil biozones, and species ranges of planktic foraminifera, calcareous nannofossils, and macrofossils at the North El Qasr section.

presence of *Braarudosphaera bigelowii* and *A. cymbiformis* also indicates marginal marine conditions (Perch-Nielsen, 1985).

6.4. *Lower/Upper Maastrichtian boundary*

This boundary has not yet been formally defined (Odin, 1996). It is generally placed at the first appearance of the planktic foraminifera *Gansserina gansseri* (Robaszynski *et al.*, 1983–1984; Caron, 1985; Li & Keller, 1998a, b), or at the FAD of *Abathomphalus mayaroensis* or *Racemiguembelina fructicosa* (Nederbragt, 1991). However, it is well known that the FAD of *A. mayoraensis* is diachronous and occurs earlier in high latitudes (see Pardo *et al.*, 1996). Numerically, the early/late Maastrichtian boundary has been placed at 69.5 Ma within the upper part of C31R (Gradstein *et al.*, 1995), an interval that corresponds to the FAD of *R. contusa* (=base of CF6, Li & Keller 1998a). Li *et al.* (1999) used the FAD of *R. fructicosa* to approximate the early/late Maastrichtian boundary at 68.2 Ma based on biostratigraphic correlation with the geomagnetic time scale at DSDP Site 525. Calcareous nannofossil workers generally place this boundary at the base of the *A. cymbiformis* Zone (CC25, e.g., Sissingh, 1977; Roth, 1978; Perch-Nielsen, 1985), which corresponds to the base of CF6 (Figure 3). In this study we follow Gradstein *et al.* (1995) and Li & Keller (1998a, b) by using the FAD of *R. contusa* at 69.56 Ma as a marker species for the early/late Maastrichtian boundary. This datum event coincides with the FAD of the calcareous nannofossil *L. quadratus* (base of zone CC25b) that is employed by many workers as marker for this boundary (Bralower *et al.*, 1995). In the Gebel Gifata section, the early/late Maastrichtian boundary occurs within the middle part of the Beris Mudstone Member of the Dakhla Formation.

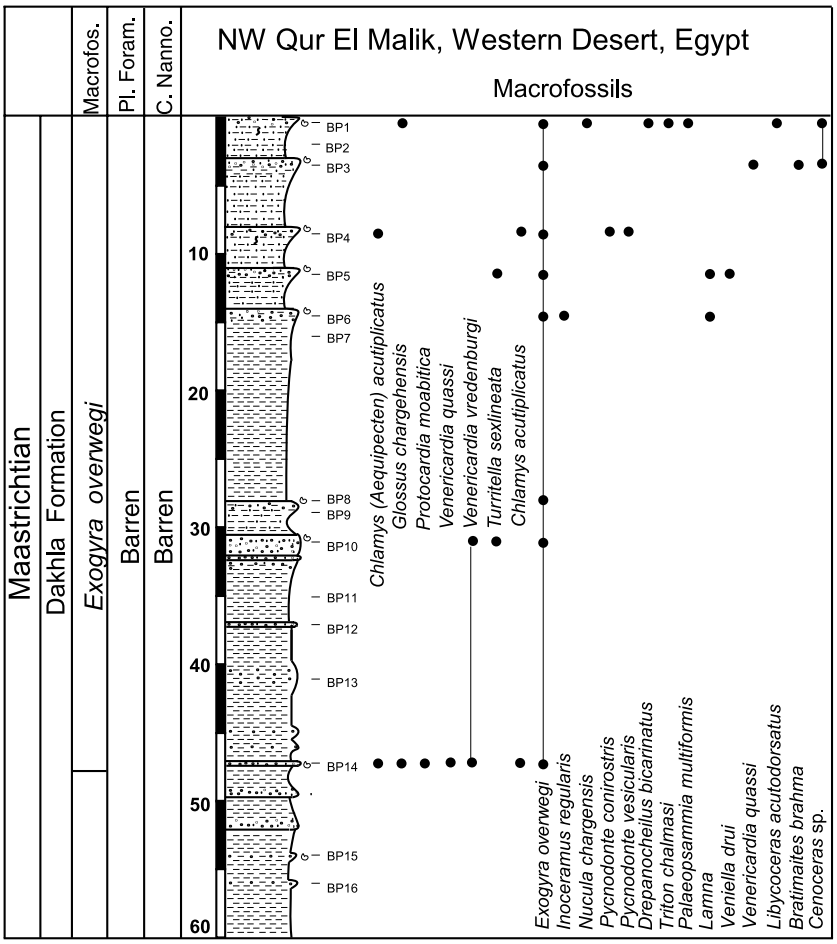

Figure 11. Lithological column, macrofossil ranges, and biozones at the Northwest Qur El Malik section. This section does not contain any microfossils.

6.5. *Upper Maastrichtian*

At Gebel Gifata two 1-m-thick calcareous sandstone layers, located in the interval between 96 m and 103 m, contain low-diversity upper Maastrichtian planktic foraminiferal assemblages consisting of shallow-water or surface-dwelling species (Figure 4). We tentatively place these species assemblages within zone CF6 because of the presence of common rugoglobigerinids. The index species *Rosita contusa* first appears at 103 m. A zone CF6 age is also suggested by the presence of the calcareous nannofossil species *L. quadratus* that marks the base of the *L. quadratus* Zone (CC25b; Figure 4). The nannofossil assemblages are similar, but relatively less diverse than those of the underlying zone CC25a. Deposition of these microfossil assemblages probably occurred in an inner neritic environment, as suggested by generally lower species diversity and absence of deeper dwelling globotruncanid species. The presence of abundant macrofossils, vertebrate bones (Figure 3), Fe-rich sand and very abundant benthic foraminifera (*c.* 95% relative to planktic foraminifera) indicates that deposition occurred in a very shallow, high-energy, inner neritic to littoral environment. The overlying 17 m of shale are devoid of microfossils and only rare macrofossils are present, such as small nuculanid and pectinic bivalves that suggest dysaerobic conditions.

At Bir Abu Minqar zone CF6 planktic foraminiferal assemblages are tentatively identified in calcareous sandstone layers although the index species *Rosita contusa* was not observed (Figure 9). A major hiatus is present at this interval with early Paleocene zone P1d above the early late Maastrichtian zone CF6. Macrofossils present in the calcareous sandstone layer below the hiatus include *Baculites anceps*, *B. vertebralis*, *Eutrephoceras* sp., *Glyptoxoceras* sp. and *Hercoglossa* aff. *danica*. The presence of the Danian species *H.* aff. *danica* indicates that early Tertiary nautilids are mixed with Maastrichtian faunal elements at this hiatus.

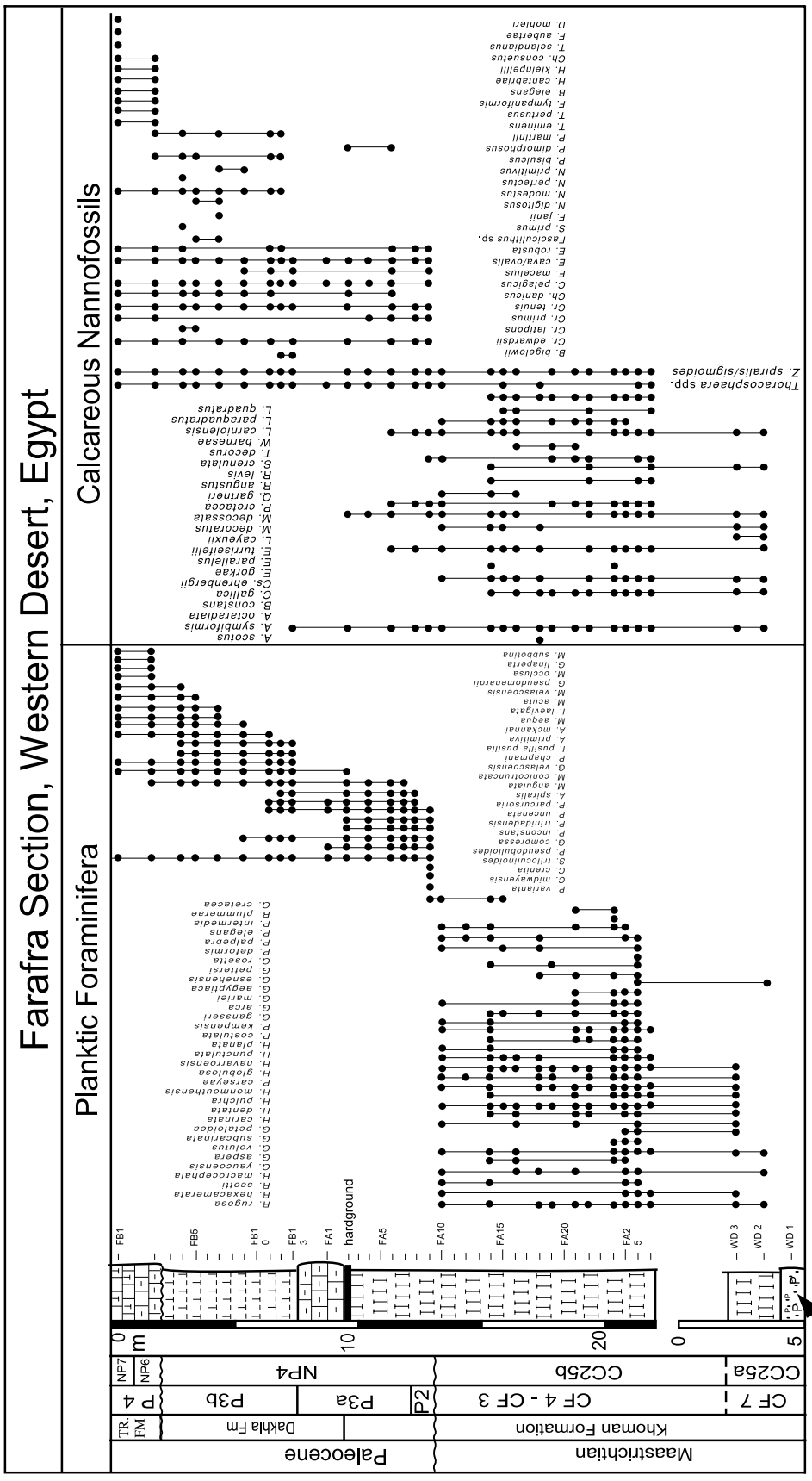

Figure 12. Lithological column and planktic foraminiferal and calcareous nannofossil species ranges and biozones at the Farafra section, located about 15 km north of Qasr El Farafra at the North Gunna locality that is marked by a group of three isolated conical hills. The basal part of the section was sampled in the White Desert, about 25 km to the north.

In the upper part of the Beris Mudstone Member at Gebel Gifata, two graded shell hash beds are present between 120–122.5 and 126.5–127.5 m with mud-clasts and *Thalassinoides* burrows at the base and top that mark erosional surfaces (Figure 4). Calcareous nannofossils in this interval are indicative of the upper zone CC25b (*M. decussata/concava*, *W. barnesae*, *P. cretacea*, *A. cymbiformis*, *L. quadratus*, *C. ehrenbergii*, *E. turriseiffelii* and *P. stoveri*; Figure 4). Only rare planktic foraminifera are at the base of these shell hash beds (e.g., *H. globulosa*, *P. carseyae*, *A. blowi*, *A. cretacea*, *R. rugosa*; Figure 4). However, near the top of the shell hash are more diverse assemblages, including *Gansserina aegyptiaca*, *G. gansseri*, *P. carseyae*, *P. costulata*, *P. deformis*, *P. elegans*, *H. globulosa*, *H. punctulata*, *R. rugosa* and *A. cretacea*. Although the zone CF4 index species (*Abathomphalus mayaroensis* or *Racemiguembelina fructicosa*) are absent, the presence of relatively common *G. gansseri* within these assemblages suggests a CF4 age that corresponds to the upper part of CC25b (Figures 4, 8). *Gansserina gansseri* has been observed to reappear in significant abundance (*c.* 10-15%) near the top of its range within CF4 (Li & Keller, 1998a, b; Abramovich *et al.*, 1998). Similar assemblages were observed at North El Qasr, in two sandstone beds near the top of the section (Figure 10). At Bir Abu Minquar the interval from the upper Maastrichtian zone CF6 through the lower Danian is missing owing to a hiatus (Figure 9).

The predominance of benthic foraminifera (>95%) in these two shell hash beds suggests that deposition occurred within a shallow, high-energy, inner neritic to littoral environment, with either periodic marine incursions transporting open marine planktic foraminiferal assemblages into the coastal areas, or reworking and transport. The former is indicated by the excellent preservation of planktic foraminifera and absence of broken or abraided shells that would be expected if the assemblages were reworked and transported in a high-energy environment. The dark grey silt between these two shell hash beds is devoid of microfossils, similar to the barren intervals below and above, and suggests that deposition alternated between neritic and lagoonal to brackish environments.

At Farafra, the same statigraphic interval was deposited in a deeper middle neritic environment, as indicated by the diverse foraminiferal assemblages and chalk deposition (Figure 12). At this locality, the lower 7 m of the exposed outcrop contain assemblages that suggest a CF4–CF3 age, though the zonal index species (*A. mayaroensis*, *R. fructicosa*, *P. hariaensis*) are not present probably owing to the shallow depth of deposition of this succession. However, a CF4 assemblage is indicated near the base of the section by the presence of *R. plummerae*, which disappeared within CF4, and a CF3 assemblage is indicated by the disappearance of *G. gansseri* in sample FA14, that marks the top of CF3 (Figure 12). Well-preserved and diverse upper Maastrichtian calcareous nannofossils indicative of zone CC25b are present in this interval.

At Gebel Gifata, the Lower Kharga Shale Member of the Dakhla Formation consists of dark grey shale that is barren of microfossils, but contains fish scales, callianassid pincers, and rare bivalves indicating a shallow marine environment (Figure 3). Other invertebrate fossils are rare and restricted to nuculanid and pectinid bivalves, and an isolated fragment of a scaphitid ammonite (sample DL20). At the top of this interval, a 1-m-thick calcareous shale (samples DL3–DL1) contains a low-diversity solution-resistant calcareous nannofossil assemblage indicative of zone CC26a, including the index species *Micula murus* (Figure 4). A low-diversity, shallow-water, late Maastrichtian planktonic foraminiferal assemblage is present and dominated by *H. dendata*, *H. globulosa*, *H. navarroensis* and *Guembelitria cretacea*, as well as abundant benthic foraminifera (*c.* 65%) and common macrofossils (e.g., *Veniella drui*, *V. quassi*, *Chlamys* sp., *Lithophaga*). All of these fossils indicate that deposition occurred in an inner neritic environment. Although there are no age-diagnostic species present, the common presence of *G. cretacea* along with small biserial taxa suggests a CF3 age characterized by a *Guembelitria* acme in the eastern Tethys (Abramovich *et al.*, 1998).

6.6. *Cretaceous/Tertiary transition*

The K/T boundary is marked by a major hiatus in all of the sections examined. At Gebel Gifata, a pronounced erosional surface marks a hiatus between the top of the dark grey shale (Lower Kharga Shale Unit) and the overlying 25-cm-thick yellow calcareous sandstone that marks the base of the Bir Abu Minqar horizon. The calcareous sandstone and overlying siltstone (samples DK2, DK3) contain rounded quartz grains, phosphate nodules, glauconite and abraded benthic foraminifera. An early Danian planktic foraminiferal zone P1c assemblage is present and consists of *Guembelitria cretacea*, *Globoconusa daubjergensis*, *Woodringina hornerstownensis*, *W. claytonensis*, *Parasubbotina pseudobulloides*, *Subbotina triloculinoides* and *Chiloguembelina kelleri* (Figure 7). Rare biserial Cretaceous species are also present (*H. globulosa*). Sample DK3 contains a low-diversity calcareous nannofossil assemblage which consists of *Cruciplacolithus primus*, *C. tenuis*, *Prinsius martinii*, *P. dimorphosus* and *Neochiastozygus primitivus*, as well as common

Cretaceous survivor species (Figure 7). This assemblage is indicative of the early Danian zone NP2, which is equivalent to planktic foraminiferal zone P1c (Figures 7, 8). Similarly, the presence of abundant macrofossil species *Venericardia libyca* (Zittel) indicates the *Venericardia libyca* Zone of Danian age (e.g., Kassab & Zakhera, 1995; Figure 3). Most of the macrofossil specimens are isolated shells that indicate transport, but in pockets near the base of the sandstone layer many specimens are still closed and may represent little-transported or autochthonous assemblages. Thus, micro- and macrofossil assemblages indicate the presence of a major hiatus at the K/T transition, as indicated by the juxtaposition of the calcareous nannofossil zones CC25a and NP2, as well as the planktic foraminiferal zones CF3 and P1c at Gebel Gifata, and the overlying Danian *Venericardia libyca* (macrofossil) zone. This hiatus spans about 1 m.y. (64.5–65.5 Ma) from the lower Danian planktonic foraminiferal zone Plc and calcareous nannofossil zone NP1 through the uppermost Maastrichtian zone CF2 or CC26b (*M. prinsii* zone; Figures 7, 8).

Major K/T hiatuses are also present at other Western Desert sections. At Bir Abu Minquar the K/T hiatus spans from the Danian zone P1d–P2 or NP4 to the early late Maastrichtian zone CF6 or CC25b (*c.* 61–69 Ma; Figure 9). At Farafra the K/T hiatus spans the Danian zone P2 and NP4 to the early late Maastrichtian CF3–CF4 and CC25b (*c.* 61–66 Ma; Figure 12). A hiatus of this magnitude was also reported by Samir (1995), although his *G. gansseri* Zone (Caron, 1985) encompasses our zones CF4–CF7 (Figure 8).

6.7. Early Paleocene

Above the K/T hiatus at Gebel Gifata, sediments contain early Danian zone Plc planktic foraminiferal assemblages characterized by few *Guembelitria cretacea* and *G. trifolia* and common *Parasubbotina pseudobulloides*, *Subbotina triloculinoides*, *Woodringina hornerstownensis*, *W. claytonensis* and *Chiloguembelina morsei* (Figure 7). A morphologically small and low-diversity benthic foraminiferal assemblage indicates a low-oxygen environment. These foraminifera suggest that sediment deposition occurred within a low-energy, low-oxygen middle neritic environment. Calcareous nannofossils in this interval also contain a low-diversity assemblage with low-species abundances. Only five Danian species (*Cruciplacolithus primus*, *C. tenuis*, *P. martinii*, *P. dimorphosus* and *N. primitivus*) characteristic of zone NP2, and two survivor species (*Thoracosphaera operculata* and *B. begelowii*) are present. The presence of the latter species supports deposition in a neritic environment. In addition, *Venericardia libyca*, *Nucula chargensis* and *Nuculana protexta* are present and suggest low-oxygen shallow-water conditions (Figure 3).

At 10 m above the K/T boundary at Gebel Gifata is a 40-cm-thick limestone with mudclasts at its base (Figure 4). The upper part has a sugary texture, is rich in glauconite, and underlies a thin glauconite layer. Foraminifera are rare and poorly preserved owing to dissolution. Species identified include *Praemurica inconstans*, *Planorotalites compressa*, *W. hornerstownensis*, *S. triloculinoides* and *G. cretacea*, which indicate an upper zone Plc(2) faunal assemblage. Above the glauconite is another 40-cm-thick limestone layer with a similar planktic foraminiferal assemblage (*P. pseudobulloides*, *P. varianta*, *S. triloculinoides*). A 50-cm-thick glauconite layer disconformably overlies the limestone and contains a diverse Plc(2) assemblage with abundant planktic foraminifera (Figure 7).

The marly shales above the glauconite layer are rich in planktic foraminifera, including common *Morozovella trinidadensis*, *Praemurica inconstans*, abundant *P. compressa*, *P. pseudobulloides*, *P. varianta*, *G. daubjergensis*, and few *C. midwayensis*. *Praemurica taurica* and *P. pentagona* are conspicuously absent. This assemblage indicates a zone Pld age. Nannofossils in this interval indicate a zone NP4 age (Figure 7). Benthic foraminifera are rare (*c.* 10%), relative to planktic foraminifera (*c.* 90%). The low benthic/planktic ratio, high abundance of planktic foraminifera, and absence of coarse detrital influx in the sediment indicate a deeper middle to outer neritic, open marine environment.

From 11 m above the K/T boundary up to the top of the section, there is a notable increase in abundance and diversity of calcareous nannofossil species that is characteristic of zone NP4 (Eshet *et al.*, 1992; Figure 7). The calcareous survivor species are also present and include *B. bigelowii*, *Thoracosphaera* spp., and *Zygodiscus sigmoides*. Similar nannofossil assemblages are present at Bir Abu Minqar between samples AM2 and AM3, and also indicate a NP4 age (Figure 9). Below this horizon (sample AM4) are diverse mixed Maastrichtian and Danian planktic foraminiferal assemblages in a glauconitic calcareous sandstone that disconformably overlies Maastrichtian shale. Danian planktic foraminifera within this mixed assemblage indicate a zone P1d age, and reworked Maastrichtian species indicative of zone CF6 are present. The presence of the Danian nautilid *Hercoglossa danica* also suggests faunal mixing. Thus erosion at Bir Abu Minquar during the early Danian removed the K/T boundary and late Maastrichtian intervals (Figure 9).

Strong erosion during the Danian is also evidenced at Farafra where a P2 planktic foraminiferal assemblage and a lower zone NP4 calcareous nannofossil assemblage overlie late Maastrichtian zone CF4–3 and CC25b assemblages (Figure 12). Above this erosion surface, the assemblages change to P3a with the first appearance of *M. angulata*, followed by zone P3b with the appearance of *G. velascoensis*, *P. chapmani*, and *Igorina pusilla*. These foraminiferal assemblages mark the Selandian, as also indicated by the presence of the NP4 calcareous nannofossil assemblage (e.g., *Cruciplacolithus edwardsii*, *C. danicus*, *C. primus*, *C. tenuis*, *E. macellus*, *C. pelagicus*, *E. cava/ovalis*, *E. robusta*, *F. janii*, *N. modestus*, and *P. dimorphosus*). At the top of the outcrop a zone P4 (Thanetian) assemblage is present, as marked by the presence of *G. pseudomenardii*, *M. velascoensis*, *M. occlusa*, and *M. subbotina* (Figure 12). Age equivalent Thanetian calcareous nannofossil assemblages are represented by zones NP6 and NP7. The upper parts of zones NP4 and NP5 are missing and mark a distinct hiatus between the Dakhla and Tarawan formations.

7. Mineralogy and geochemistry of the Gebel Gifata section

Sediments at Gebel Gifata are dominated by phyllosilicates (40–80%). Calcite is present only in the Duwi Formation and in calcareous sandstone layers (20–80%) of the Dakhla Formation (Figure 13). Feldspar (plagioclase) and anhydrite (late diagenetic product linked to arid climate; Chamley, 1989) are minor constituents (0–5%), though generally more abundant in the lower part of the section. Quartz is nearly absent in the lower 30 m of the section, but gradually increases to a maximum of 40% at the top of the Mawhood Shale Member, coincident with the base of the *Exogyra overwegi* Zone. Quartz enrichment at this stratigraphic horizon was also observed at the Northwest Qur El Malik section. Above this interval, quartz is a minor constituent with peaks (10–15%) in thin sandy layers, except for the Upper Kharga Shale Member at the top of the section. Maximum detrital influx thus occurred during deposition of the lower Maastrichtian zone CF7 at Gebel Gifata and Northwest Qur El Malik, and suggests uplift and subsequent erosion to the southwest. The presence of the *Exogyra overwegi* marker horizon in these sections indicates shallowing, possibly linked to uplift of the Gilf El Kebir Spur (Barthel & Hermann-Degen, 1981) and/or falling sea level.

The main clay phases at Gebel Gifata are kaolinite (30–80%), smectite (10–60%), chlorite (0–30%) and mica (0–10%). The constant presence of smectite indicates the absence of a strong diagenetic overprint owing to burial, as also suggested by the low temperature value of the S2 peak that indicates immature organic matter. The smectite presence also implies a detrital origin that may reflect local uplift and/or variations in weathering processes and soil formation in the bordering continental areas (Chamley, 1989; Weaver, 1989). Kaolinite increased from 40–60% at the base of the section (CF8 zone) to 60–80% in CF4, and reached a maximum abundance of 80–90% in the uppermost part of the section that spans the late Maastrichtian–early Danian (CF3–P1c interval; Figures 14, 15).

During the Late Cretaceous, the section at Gebel Gifata was near the palaeoequator (Smith *et al.*, 1982). An equatorial position is also indicated by the high abundance of kaolinite, which suggests warm wet, tropical and subtropical conditions characterized by low seasonality contrasts, and predominantly chemical weathering (high kaolinite and smectite, very low mica and chlorite contents). The increase in kaolinite towards the K/T transition was also observed in Tunisia (Keller *et al.*, 1998; Li *et al.*, 2000; Adatte *et al.*, in press), and suggests a change towards more humid conditions with enhanced runoff. Tropical to subtropical environmental conditions are also indicated by the presence of the mangrove palm *Nypa* (pollen grains *Spinizonocolpites*, *Proxapertites*) and their fruit in the early Danian zone P1d at Bir Abu Minqar (Figure 9; Schrank, 1984, 1987; Ganz *et al.*, 1990b). Today, *Nypa* mangroves thrive in humid tropical swamps, estuaries and tidal shores. Their presence in the Dakhla shale thus indicates a warm, humid climate and proximity to land. Moreover, the presence of the pollen grain *Tricolpites reticulatus*, which is comparable to products of extant *Gunnera* that is restricted to environments of heavy rainfall and higher altitudes (>750 m), indicates significant elevation nearby with heavy rainfall during the Late Maastrichtian–early Danian (Schrank, 1984).

8. Cyclic deposition

Cyclic deposition of alternating calcareous sandstones and shales at Gebel Gifata has been analyzed for four stratigraphic horizons (*Exogyra overwegi* Zone, upper CF7, CF4, and K/T transition CF3–P1c). The calcareous sandstone-shale cycles are characterized by significant differences in clay mineral abundances, except for chlorite and mica, which show similar patterns in both lithologies (average 11 and 6% in sandstone layers, and 5 and 3% in shale layers

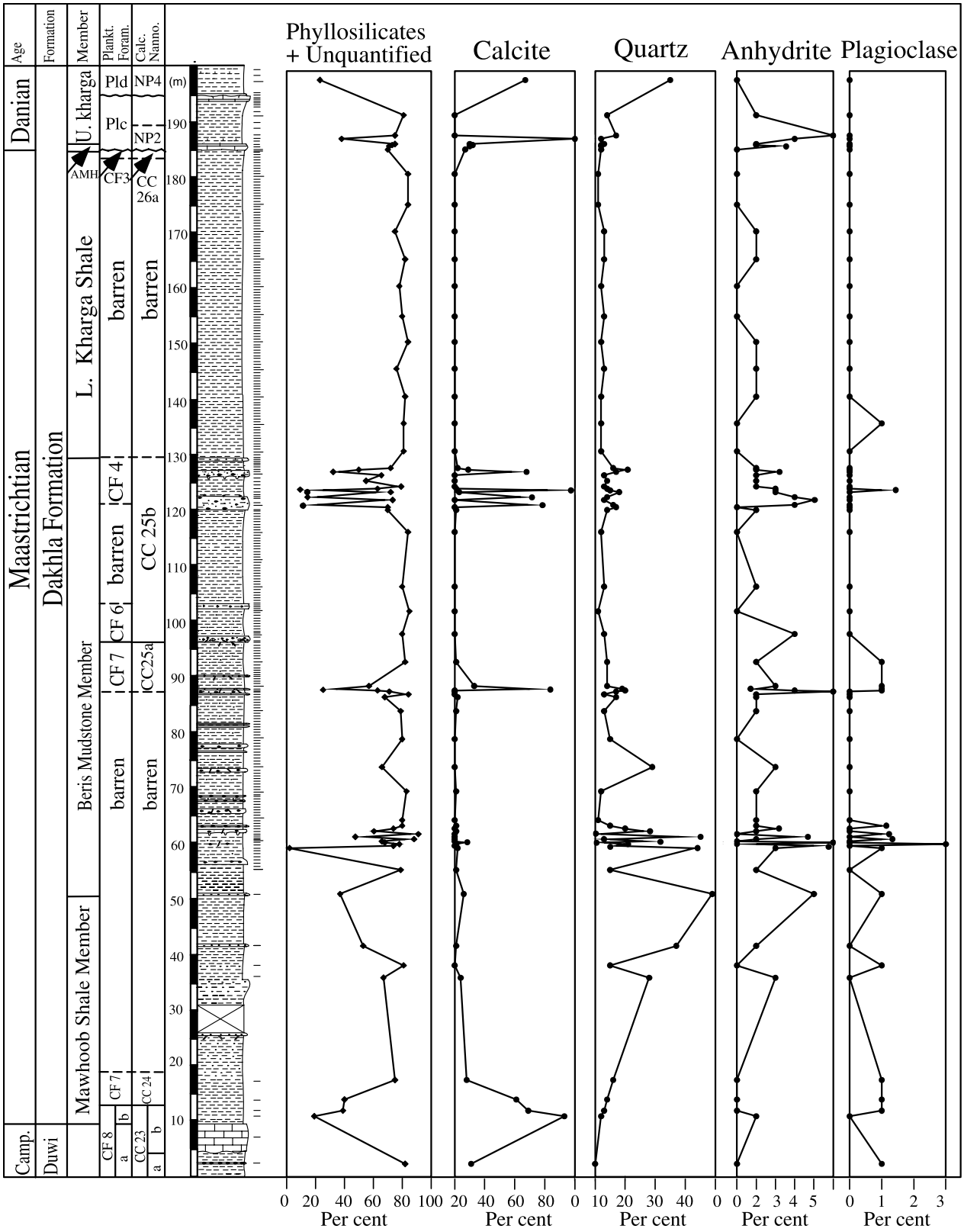

Figure 13. Bulk rock composition of the Dakhla Formation at Gebel Gifata. The maximum terrigenous influx occurred during deposition of the Mawhoob Shale Member in the early Maastrichtian, suggesting subsidence of the Dakhla Basin.

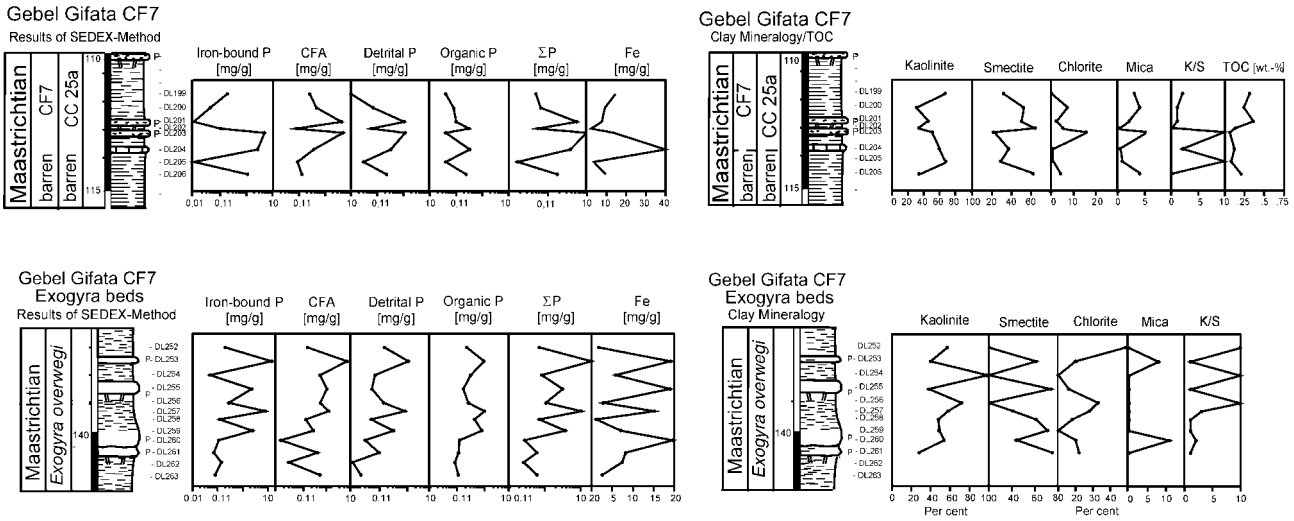

Figure 14. Clay mineralogy and geochemistry of two sedimentary cycles in the early Maastrichtian zone CF7: *Exogyra* beds in the lower part of planktic foraminiferal zone CF7, and the upper part of CF7, and calcareous nannofossil zone CC25a; see text for discussion.

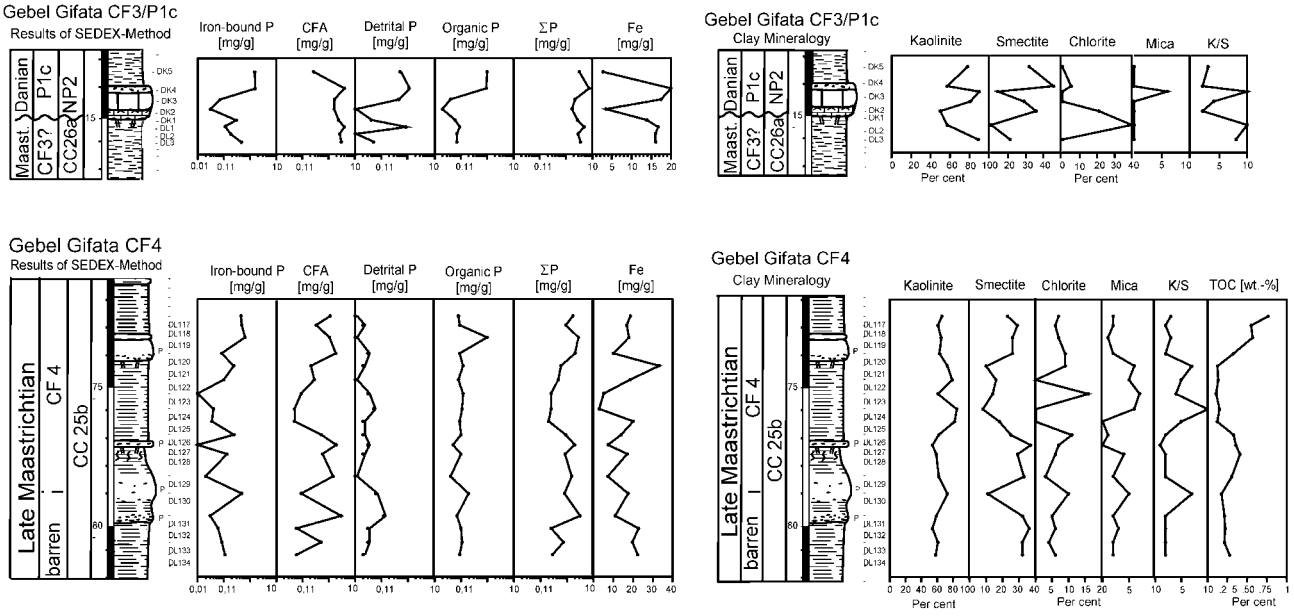

Figure 15. Clay mineralogy and geochemistry of two sedimentary cycles in the late Maastrichtian planktic foraminiferal zone CF4 and calcareous nannofossil zone CC25b, and the K/T transition (CF3/Plc and CC26a/NP2); see text for discussion.

respectively). In general, kaolinite is more abundant in shale intervals than in calcareous sandstone layers (average 63 and 50% respectively), whereas smectite is more abundant in calcareous sandstones than in shales (average 33 and 29% respectively, Figures 14, 15). This represents an inverse trend since smectite is generally more abundant in shales, indicating periods of sea-level high-stands and more open environments, whereas kaolinite is generally more common in calcareous sandstone representing near-shore conditions (Chamley, 1989; Chamley *et al.*, 1990). In the cyclic deposition at Gebel Gifata, smectite in shales is generally transformed into chlorite-like phyllosilicates (chlorite-smectite mixed layers). This diagenetic alteration compromises the K/S ratio as an indicator of original climate and sea-level variations. The observed inverse trend in smectite can be explained by degradation and partial destruction of smectite by organic acids under strongly reducing conditions (Chamley, 1989). This clay degradation in

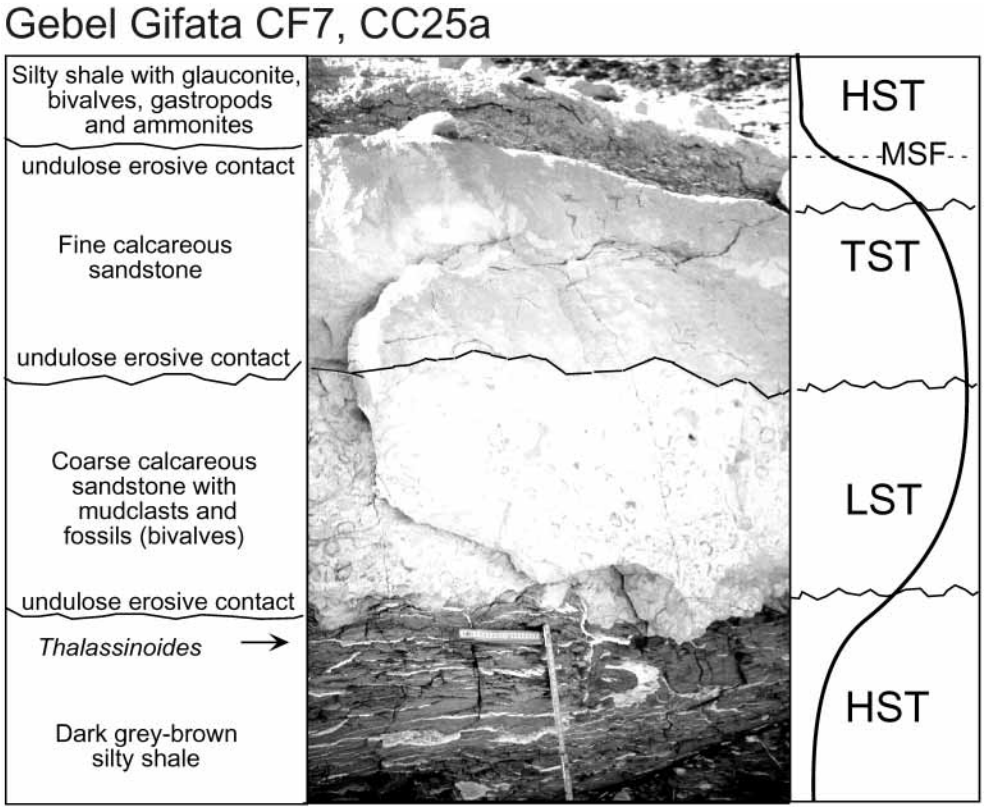

Figure 16. Sequence stratigraphy and sea-level changes across the shale/calcareous sandstone cycle near the top of planktic foraminiferal zone CF7 and calcareous nannofossil zone CC25a. The undulating erosional surfaces between the dark shales and calcareous sandstone layers and between the fine- and coarse-grained calcareous sandstone layers mark sea-level changes.

black shales probably occurred close to the sediment-water interface. Under such conditions, smectite preferentially degrades into a chlorite-smectite mixed layer, or chlorite-like mineral, whereas the more resistant kaolinite is preferentially preserved.

Clues to the nature and variation of cyclic sediment deposition at Gebel Gifata can be gleaned from thin sections. Near the base of the section (sample DL280), abundant phosphatic bioclasts and lithoclasts are present in a poorly sorted layer that contains phosphatic fish bones and scales, teeth, lithoclasts, faecal pellets, rare benthic foraminifers, and varying amounts of sand and silt-sized quartz. No ooids or oncoids have been observed. The iron-stained micritic (phosphatic?) matrix is frequently dolomitic. Cyclic deposition of the early Maastrichtian *Exogyra overwegi* and upper CF7 zones (Figures 14, 16) is marked by silt-rich shales and bioclastic sandstones with phosphatic bioclasts consisting mainly of fish remains (scales, bones and teeth). The non-phosphatic fraction increased, including abundant planktic and benthic foraminifera and minor amounts of silty detritus. In addition, hematite and goethite grains or coatings are frequently present, though no phosphatic matrix was observed. Cyclic deposition in the upper Maastrichtian–lower Paleocene (samples DL130 to DK18; Figure 15), is characterized by micritic shales and bioclastic sandstones with shell-rich intervals and phosphatic lithoclasts and glauconite at the top of the cycles. The latter two are presumably of authigenic and peloidal origin, as suggested by their typically mammilate to lobate-shaped form and absence of distinct internal structure.

Organic carbon and Rock-Eval pyrolysis data indicate that total organic carbon (TOC) values are generally very low and rarely exceed 0.5 wt.%, with average values about 0.25 wt.% (Figures 14, 15). Higher values are generally associated with hardgrounds and hiatuses. All of the kerogens present are thermally immature, as indicated by the low to slightly elevated temperature maximum (Tmax) values of 435–451°C. The pyrolysis-data further suggest a terrigenous source (Type III or IV), high sediment dilution, and perhaps oxidizing bottom conditions. However, post-depositional alteration is also

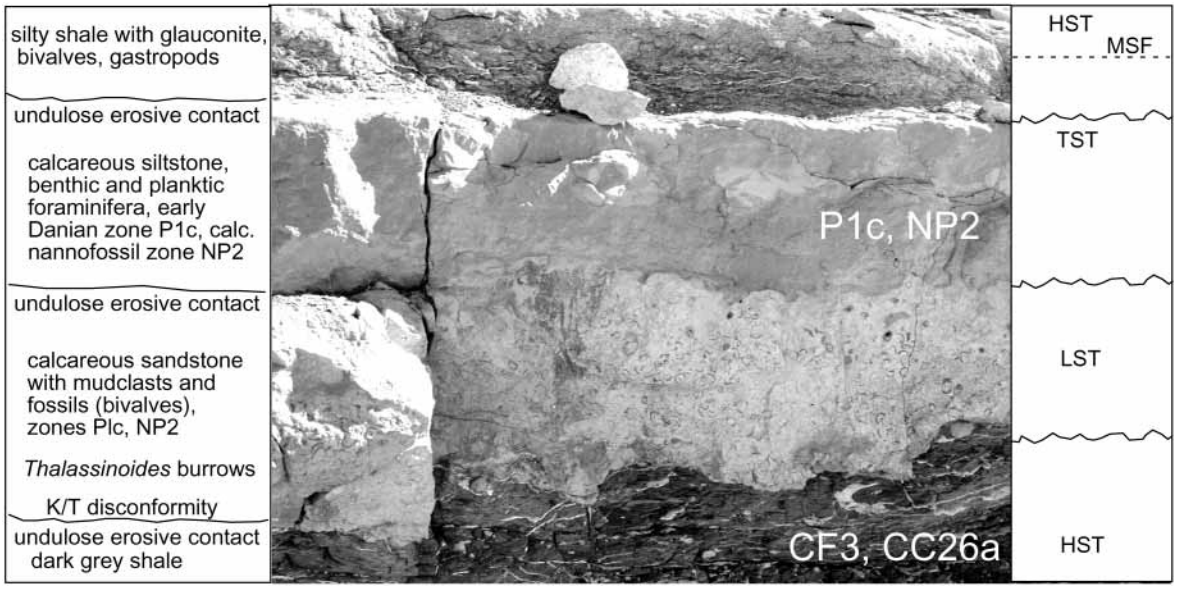

Figure 17. Sequence stratigraphy and sea-level changes across the Cretaceous/Tertiary boundary disconformity at Gebel Gifata. The disconformity juxtaposes the late Maastrichtian planktic foraminiferal zone CF3 and calcareous nannofossil zone CC26a with the early Danian Bir Abu Minqar horizon of planktic foraminiferal zone Plc and calcareous nannofossil zone NP2 age. The undulating erosional surfaces between the dark shale and calcareous sandstone layers at the top and bottom, and within the calcareous sandstone layer mark changes in sea levels.

indicated by the low hydrogen index (HI) (30–40 HC/g TOC) and extraordinarily high oxygen index (OI) (200–580 mg CO_2/g TOC) values. This indicates that the main part of the organic matter in the shale has been altered and destroyed.

Phosphorus (P) concentrations of the different P-bearing phases reveal highly variable patterns throughout the four cyclic intervals of the Dakhla section analyzed, although no larger general trends in the P-geochemistry are apparent (Figures 14, 15). Therefore, major variations in the P-concentrations are confined to the lithologic changes from phosphate-poor shale (<0.1 mg/g total P) to the more P-enriched bioclastic calcareous sandstone beds (0.5–5 mg/g total P), although P-concentrations can also be increased in adjacent shales. The elevated P contents of bioclastic sandstone beds are derived mainly from the higher calcium fluor apatite (CFA) (up to 5 mg/g) and detrital P values (up to 0.1 mg/g), whereas organic P (about 0.1 mg/g) shows no major changes, and iron-bound P values are highly irregular (<0.1 to 1 mg/g). Since phosphate from the CFA phase is associated mainly with authigenic P-rich minerals and secondarily with biogenic apatite debris (e.g., fish teeth and bones), these results confirm the observations from thin-section studies that reveal biogenic apatite debris as the main source of phosphate. In addition, elevated detrital P values, equivalent to detrital (igneous/metamorphic) fluor apatite and residual phases, argue for a condensed/winnowed or reworked origin of these beds. The unusual high iron-content (with up to 40 mg/g) points to a high fluvial input as also suggested by the high phyllosilicate kaolinite contents.

9. Sequence stratigraphy of cycles

The 23 calcareous sandstone-shale cycles identified in the Gebel Gifata section exhibit similar features. Two representative examples from the lower Maastrichtian (upper part of zones CF7 and CC25a) and the K/T transition (CF3–P1c; Figures 16, 17) show similar lithologies, disconformities and microfacies. In each cycle, the dark silty shales represent sea-level highstands, whereas the calcareous sandstones represent sea-level lowstand periods, as suggested by the lithologies, fossil content, and erosional surfaces. The monotonous dark grey silty shales are generally barren of microfossils. Deposition of this succession occurred during sea-level highstands in restricted inner neritic to lagoonal environments characterized by euryhaline, dysaerobic, or low oxygen conditions probably related to a stagnating sea. The contact between the shale and the overlying calcareous sandstone is generally marked by an undulating erosional surface (Figures 16, 17).

Above this erosive contact, the lower part of the calcareous sandstone is coarse-grained, strongly bioturbated, and generally consists of accumulated bivalves, other fossil debris and occasional wood fragments that reflect high hydrodynamic conditions (tempestite). These coarse-grained sediments may represent sandbars deposited in well-oxygenated shallow waters during sea-level lowstand (LST) periods. The upper part of the calcareous sandstone is generally finer grained and overlies an undulating surface that is interpreted as a sea-level rise (transgressive system track, TST). The glauconitic and/or phosphatic silty-shale layer enriched with marine plankton that generally overlies this interval (Figures 16, 17) represents a period of condensed sedimentation and maximum influx of terrestrial organic matter that corresponds to a maximum flooding surface (MSF). The overlying shale represents a sea-level highstand (HST) period; microplankton are generally very rare or absent, probably as a result of inhospitable conditions owing to stagnation.

10. Discussion

10.1. Age and hiatuses

The relative ages and hiatuses of five sections in the Western Desert between Dakhla and Farafra were determined based on high-resolution sample analysis and biostratigraphic integration of planktic foraminifera, calcareous nannofossils and macrofossils. This approach provided improved biostratigraphic control and more accurate determination of the extent of hiatuses than has previously been achieved (Figure 18). However, the relative ages obtained are not as good as one could hope for because macrofossil and microfossil assemblages are generally restricted to calcareous sandstone layers; the shale layers are barren. Nevertheless, this study has added significantly to the age control and environmental history of the region.

A major hiatus spans the late Maastrichtian–early Paleocene interval in all sections. At Gebel Gifata this hiatus extends from about 64.5 Ma in the early Danian (zones NP1 or Plc) to about 66 Ma (within zones CC26a or CF3) in the late Maastrichtian. At North El Qasr the upper Maastrichtian is missing as at Gebel Gifata (lower Danian was not sampled). At Bir Abu Minqar and Farafra a hiatus spans from about 61 Ma in the late Danian (zone P2 or NP4) to about 66 Ma in the late Maastrichtian (zone CF3 or CC26a; Figure 18).

Our age determinations do not always agree with those published by other workers, nor are the hiatuses necessarily at the same stratigraphic levels. In most cases this is owing to the higher resolution planktic foraminiferal zonal scheme used in this study, the integration of nannofossil, foraminiferal, and macrofossil zonations, and the outcrop locality and higher sample resolution. For example, Samir (1995) placed the K/T hiatus at the Farafra section (North Gunna locality) at the base of a thick Danian limestone in the Dakhla Formation However in our section, the first Danian assemblage appears in the chalk 3 m below this limestone layer. There is a bioturbated hardground at the base of the Danian limestone that indicates erosion and/or non-deposition, but the extent of this hiatus within zone P3a could not be determined. It is possible that erosion in the sections sampled by Samir (1995) resulted in the juxtaposition of the Danian limestone and Maastrichtian chalk. In fact, we observed that erosion is variable along the hill slope of North Gunna and that the position of the hiatus can vary by several meters depending on the locality sampled. Possible confusion may arise from the use of different zonal schemes (see Figure 8). For example, Samir's (1995) *G. gansseri* Zone is not equal to the *G. gansseri* (CF7) zone of this study, but spans a much longer interval encompassed by zones CF7 to CF4 (Figure 8). Therefore, Samir's *G. gansseri* Zone could represent anything within the CF7–CF4 interval, but our study suggests that it represents the top and is most likely equivalent to our zone CF4.

10.2. Age of Dakhla Formation and its members

Our age determination for the Dakhla Formation and its members confirms that the Dakhla Formation spans the Maastrichtian and lower Paleocene. The Duwi/Dakhla Formation contact at the Gebel Gifata section is at the top of a 5-m-thick white micritic and phosphatic limestone which contains a zone CF8a (*G. aegyptiaca*) assemblage that spans 71–72.5 Ma (Li *et al.*, 1999). Thus, the Duwi/Dakhla contact at the top of this limestone is about 71 Ma. Abbas & Habib (1969) referred to this limestone as '*Isocardia chargensis* limestone' and Barthel & Herrmann-Degen (1981) called it the Qur El Malik Member of the Dakhla Formation. The Duwi/Dakhla contact coincides with a major global cooling and sea-level regression at about 71 Ma (e.g., Haq *et al.*, 1987; Barrera *et al.*, 1997; Li *et al.*, 1998a), which contributed to widespread erosion in shallow, continental-shelf environments of Tunisia (Li *et al.*, 1999) and Egypt.

The Mawhoob Shale Member spans the lower 40 m of the Dakhla Formation and its sediments are mostly

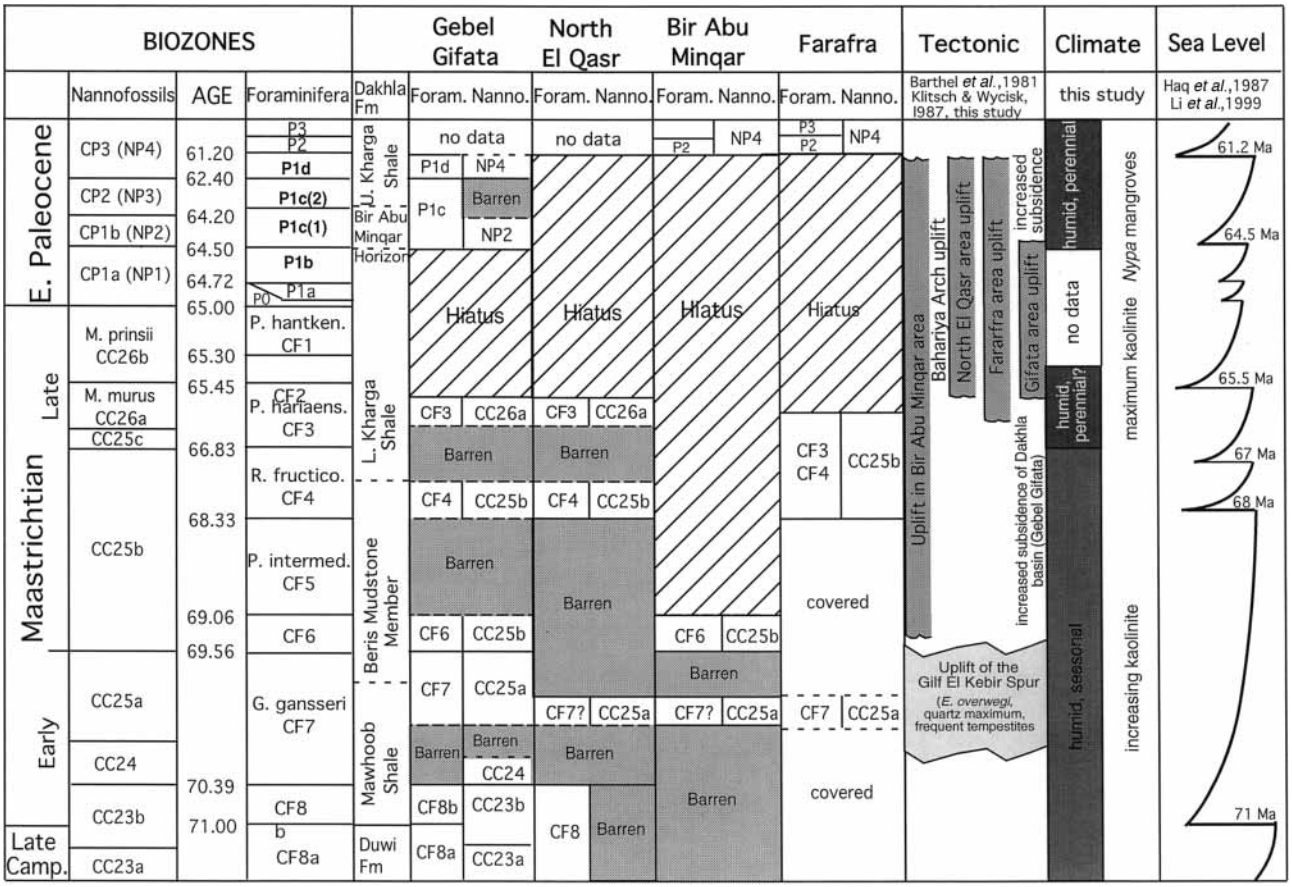

Figure 18. Stratigraphic summary, age distribution of hiatuses, barren intervals and fossiliferous horizons, tectonic activity, and climate changes inferred from clay mineralogy and fossil assemblages in the Maastrichtian–lower Paleocene (Dakhla Formation) of the Western Desert. The hiatuses are largely correlated with tectonic activity (Bahariya arch uplift) during the late Maastrichtian–early Paleocene which we estimate to have been most active between 61 and 65.5 Ma, except for the Bir Abu Minqar area where uplift began as early as 69 Ma. The coastal onlap curve of Haq *et al.* (1987) and Li *et al.* (1999, 2000) shows major sea-level lowstands at 61.2, 64.5, 65.5, and 68 Ma, which were likely contributors to the widespread erosion in the Western Desert. Climate changed from seasonally humid conditions in the early–early late Maastrichtian to perennially humid conditions during the latest Maastrichtian and early Paleocene. Ages for Paleocene zone boundaries are from Berggren *et al.* (1995) and for the Maastrichtian from Li & Keller (1998a, b; Li *et al.*, 1999).

barren of microfossils; only very rare macrofossils are present (Figure 3). The upper boundary is within the lower part of CF7 (*G. gansseri*; Figure 18). A tentative age estimate for the Mawhoob Shale is about 1 m.y. (71–70 Ma). The Beris Mudstone Member is 80 m thick and contains microfossils and macrofossils only in the calcareous sand and siltstone beds (Figures 3, 4). Planktic foraminiferal assemblages of zones CF7, CF6 and CF4 and nannofossil assemblages of zones CC25a and CC25b are present and indicate an age of about 67.5–70 Ma. This age estimate has at least a 0.5 m.y. uncertainty at the top and bottom because the upper and lower boundaries of the Beris Mudstone are within barren intervals of zones CF7 and CF4 (Figure 18).

The Lower Kharga Shale Member spans 55 m, has very few macrofossils, and is generally barren of microfossils, except for the top just below the Bir Abu Minqar horizon. A late Maastrichtian age of about 65.5 Ma (CF3, CC26a; Figure 4) is indicated for the top of the Lower Kharga Shale. A major hiatus separates this unit from the overlying Bir Abu Minqar horizon, which is of early Danian age, about 64.2–64.5 Ma, as indicated by the presence of planktic foraminiferal zone Plc(l) and nannofossil zone NP2 (Figures 4, 18). A Danian age is also indicated by the presence of *Venericardia libyca* (Kassab & Zakhira, 1995). We collected the lower 15 m of the Upper Kharga Shale, which consist of shales that are mostly barren of microfossils or macrofossils but

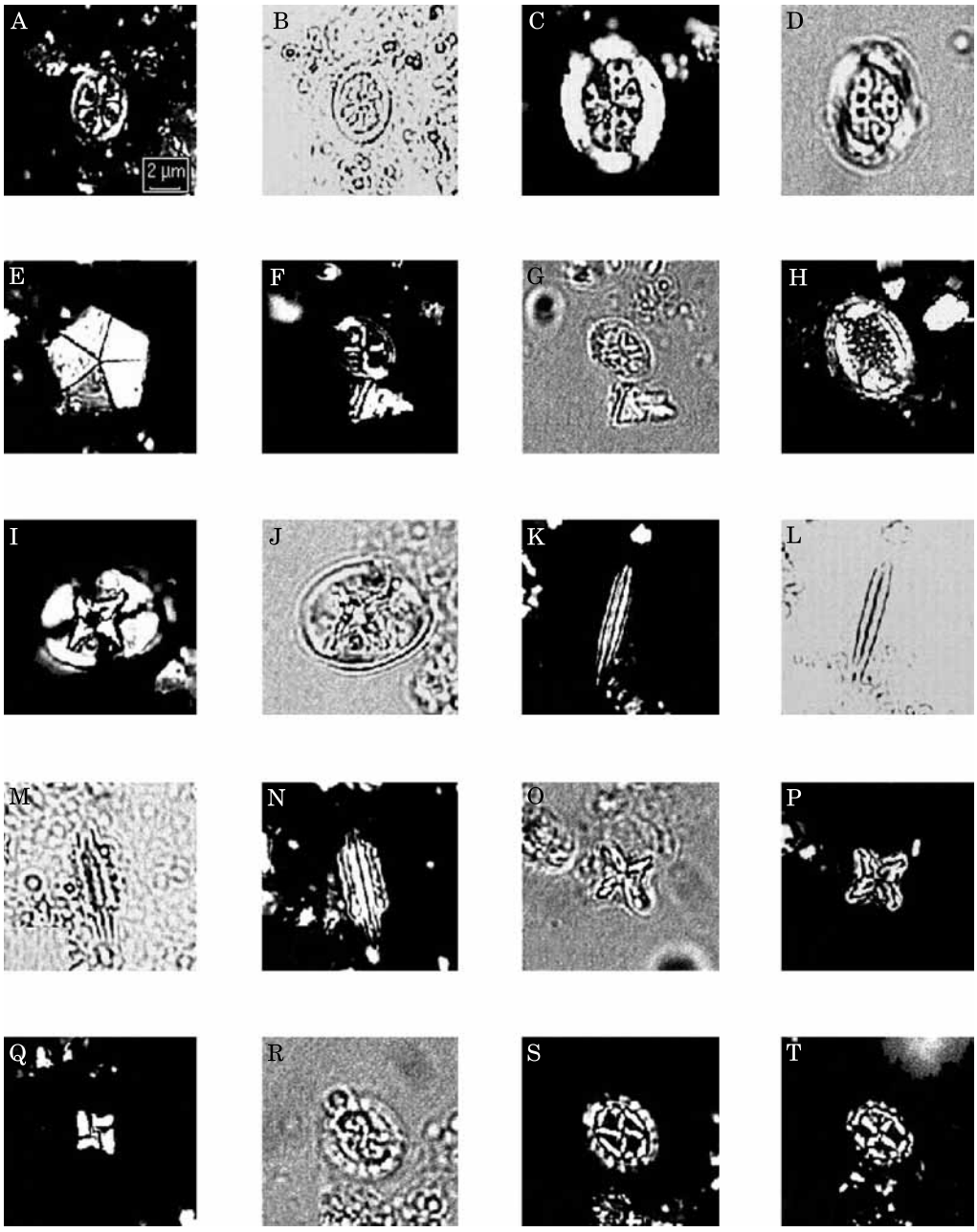

Figure 19. All illustrations are from the Gebel Gifata section. Scale bar represents about 2 µm. (XPL, cross polarized light; TL, transmitted light). A, B, *Ahmuellerella octoradiata*, sample DL181, Zone CC25b. A, XPL; B, TL. C, D, *Arkhangelskiella cymbiformis*, sample DL113, Zone CC25b. C, XPL; D, TL. E, *Braarudosphaera bigelowii*, DK22, Zone NP4, XPL. F, G, *Chiastozygus amphipons*, sample DL169, Zone CC25b. F, XPL; G, TL. H, *Cribrosphaerella ehrenbergii*, sample 131, Zone CC25b, XPL. I, J, *Eiffellithus turriseiffelii*, sample DL113, Zone CC25b. I, XPL; J, TL. K, L, *Lithraphidites carniolensis*, sample DL196, Zone CC25a. K, XPL; L, TL. M, N, *Lithraphidites quadratus*, sample DL169, Zone CC25b. M, 13: TL; N, XPL. O, P, *Micula decussata*, sample DL169, Zone CC25b. O, TL; P, XPL. Q, *Micula murus*, sample DK1, Zone CC26a, XPL. R, S, *Prediscosphaera cretacea*, sample DL127, Zone CC25b. R, TL; S, XPL. T, *Prediscosphaera spinosa*, sample DL169, Zone CC25b, XPL.

contain discrete horizons rich in microfossils spanning planktic foraminiferal zones Plc–Pld and calcareous nannofossil zones NP2–NP4, 64.2–62 Ma (Figure 18).

10.3. Tectonic activity and sea-level changes

During the Late Cretaceous, the structural differentiation of the Northeast African Plate increased, leading to the onset of the Red Sea rifting owing to the

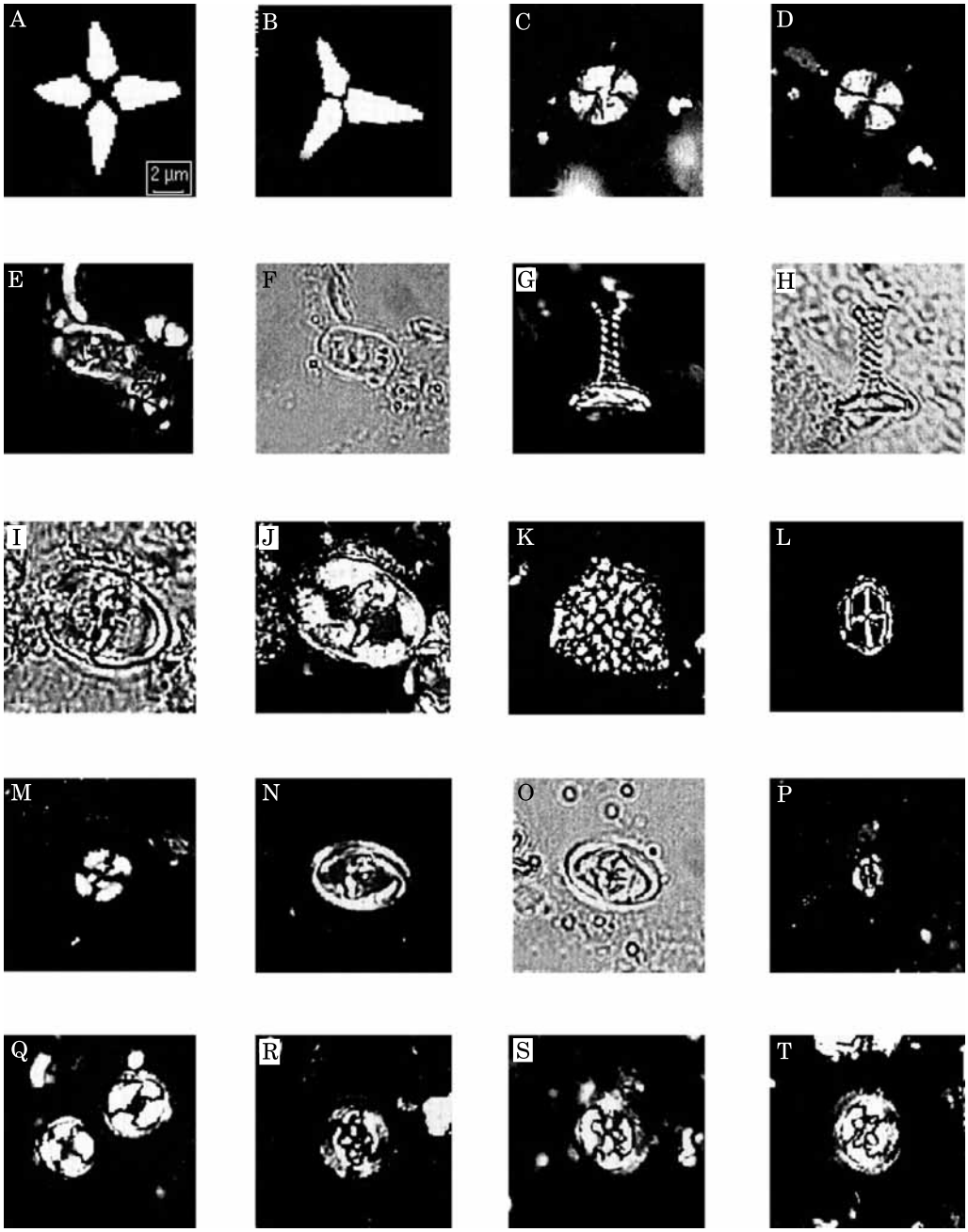

Figure 20. All illustrations from the Gebel Gifata section. Scale bar represents about 2 µm. (XPL, cross polarized light; TL, transmitted light). A, *Quadrum sissinghii*, sample DL279, Zone CC23. XPL. B, *Quadrum trifidum*, sample DL279, Zone CC23, XPL. C, D, *Reinhardtites levis*, sample DL276, Zone CC24, XPL. E, F, *Rhagodiscus angustus*, sample DL169, Zone CC25b. E, TL; F, XPL. G, H, *Podorhabdus decorus*, sample 181, Zone CC25b. G, XPL; H, TL. I, J, *Tranolithus phacelosus*, sample 169, Zone CC25b. I, TL; J, XPL. K, *Thoracosphaera* sp., sample DL195, Zone CC25a, XPL. L, *Vekshinella stradneri*, sample DL131, Zone CC25b, XPL. M, *Watznaueria barnesae*, sample DL167, Zone CC25b, XPL. N, O, *Zygodiscus sigmoides*, sample DK20, Zone NP4. N, XPL; O, TL. P, *Cruciplacolithus primus*, sample DK8, Zone NP2, XPL. Q, *Coccolithus pelagicus*, sample DK20, Zone NP4, XPL. R, *Cruciplacolithus tenuis*, sample DK22, Zone NP4, XPL. S, *Cruciplacolithus edwardsii*, sample DK22, Zone NP4, XPL. T, *Chiasomolithus danicus*, sample DK22, Zone NP4, XPL.

progressive uplift in the southern part of Egypt and a dextral strike-slip fault along the pre-existing ENE striking faults (Klitzsch, 1986). This tectonic activity reactivated the subsidence of the Paleozoic Dakhla Basin and uplift of the Kharga-Aswan Platform. In the Western Desert of Egypt, a NNW–SSE-trending relief dominated both sediment deposition and basin development during the Late Cretaceous according to Klitzsch & Wycisk (1987). Beginning in the Campanian and accelerating in the early Maastrichtian, sediment deposition was associated primarily with the Gilf El Kebir spur to the southwest of Dakhla, and the Bahariya arch that ends near the Farafra Oasis (Barthel & Hermann-Degen, 1981). The Gilf El Kebir spur acted as a source of clastic material throughout the Maastrichtian and Paleocene.

The variable depositional rates recorded for the lower and middle Maastrichtian in the Dakhla Formation of the Western Desert, and particularly in Gebel Gifata zones CF7 (8.7 cm/1000 yr) and CF4 (0.6 cm/1000 yr), strongly suggest that the depositional environment was controlled by regional tectonic activity, as well as sea-level fluctuations. Tectonic activity is indicated by peak clastic (sand) deposition during the early Maastrichtian zones CF6 and CF7, beginning just above the *Exogyra overwegi* marker horizon at Gebel Gifata (Figures 3, 9, 18), and maximum sediment deposition also occurred in the Northwest Qur El Malik area (=Ammonite Hills section of Barthel & Hermann-Degen, 1981; Figure 11), which points to a primary source from the southwest. There is significant lateral variation in sediment thickness and erosion in zones CF7–CF4 from Gebel Gifata to Bir Abu Minqar (Figures 1, 18) that may be linked to tectonic activity. The maximum sediment deposition at Gebel Gifata indicates that this locality was probably deposited at the centre of a subsiding Dakhla depression (Barthel & Hermann-Degen, 1981; Hendriks *et al.*, 1984, 1987). In contrast, decreased sediment deposition (and increased erosion) during this interval towards the northwest most likely reflects localized uplifts (e.g., Gilf El Kebir).

Minimum sediment deposition as a result of major erosion occurred during the late Maastrichtian–early Paleocene (Figure 18), with Gebel Gifata continuing to receive the highest sediment influx (Figure 1). Erosion at Gebel Gifata spans the early Danian zone Plc through the late Maastrichtian zones CF1–2 (*c.* 64.5–65.5 Ma), and increased to the northwest, reaching a maximum at Bir Abu Minqar (hiatus from CF2 to CF6, *c.* 61–69 Ma, Figure 18). A major hiatus spanning zones CF2–CF3 (*c.* 61–65.5 Ma) is also present in the Farafra area where sediment deposition occurred in a deeper middle to outer neritic environment, and a hiatus of similar magnitude was identified at the nearby Ain El Khadra section by Ibrahim & Abdel-Kireem (1997). The widespread erosion during the late Maastrichtian in the Western Desert is generally attributed to uplift of the Bahariya arch (Said, 1961; Abdel-Kireem & Samir, 1995; Galal, 1995; Abdel-Kireem *et al.*, 1996; Ibrahim & Abdel Kireem, 1997) within the Syrian arc system (Almogi-Labin *et al.*, 1990). Our study suggests that localized uplift in the Bir Abu Minqar area may have continued through the middle and late Maastrichtian, whereas at other localities uplift and erosion was restricted to the late Maastrichtian beginning about 66 Ma (Figure 18).

Although tectonic activity contributed to erosion in the Western Desert, major eustatic sea-level changes may have been the primary controlling factors for widespread erosion and hiatuses. This is indicated by the coincidence of hiatuses with known eustatic sea-level changes detailed by Haq *et al.* (1987) and Li *et al.* (1999). In addition, a study of Tunisian sections has revealed major sea-level fluctuations from the Maastrichtian through the early Paleocene (Li *et al.*, 1999, 2000), with many of the sea-level lowstands correlative with the coastal onlap curve of Haq *et al.* (1987). Major eustatic sea-level regressions occurred at about 61.2 and 64.5 Ma in the Danian, at 65.5, 67 and 68 Ma in the late Maastrichtian, and at 71 Ma at or near the Campanian/Maastrichtian boundary, as also observed in the Western Desert of Egypt (Figure 18). Additional smaller scale sea-level fluctuations occurred in the early Danian and caused widespread erosion at the P0/Pla, Pla/Plb and Plb/Plc boundaries (MacLeod & Keller, 1991; Keller & Stinnesbeck, 1996; Keller *et al.*, 1998). It is likely that major sea-level regressions were primarily responsible for the widespread erosion in the Western Desert, though local tectonic activity may have significantly contributed to local erosion and sediment deposition patterns.

11. Conclusions

1. Application of integrated biostratigraphies based on planktic foraminifera, calcareous nannofossils and macrofossils yields higher resolution age control than obtained previously for the Maastrichtian–early Paleocene Dakhla Formation of the Western Desert, Egypt. Age estimates for the Dakhla Formation and its members based on the type section at Gebel Gifata are as follows: (a) Dakhla Formation base: *c.* 71 Ma, base of planktic foraminiferal (PF) zone CF8b and lower

part of calcareous nannofossil (CN) zone CC23b, at the Duwi/Dakhla contact (El Hindawi locality); (b) Mawhoob Shale Member: *c.* 71–70 Ma, base of PF zone CF8b to upper CF7, lower part of CN zone CC23b to upper CC25a; (c) Beris Mudstone Member: *c.* 70–67.5 Ma, upper PF zone CF7 to middle CF4 and upper CN zone CC25a to upper CC25b; (d) Lower Kharga Shale: *c.* 67.5–65.5 Ma, middle PF zone CF4 to upper P1b, and upper CN zone CC25b to upper NP1; (e) Bir Abu Minqar Horizon: *c.* 64.5–64.2 Ma, PF zone Plc(l) and CN zone NP2; (f) base of Upper Kharga Shale: *c.* 64.2 Ma, base of PF zone Plc(2) and CN zone NP3.

2. Major depositional hiatuses span the upper Maastrichtian through lower Paleocene in all sections examined, though erosion generally increased from Gebel Gifata and North El Qasr (*c.* 64.5–65.5 Ma) to Bir Abu Minqar (*c.* 61.2–69 Ma). A major hiatus (*c.* 61.2–65.5 Ma) is also present in deposits of the deeper open marine environment in the Farafra area. These hiatuses appear to be linked primarily to major sea-level regressions and secondarily to regional tectonic activity (Bahariya arch uplift).

3. Variable sedimentation rates for the lower and middle Maastrichtian Dakhla Formation at Gebel Gifata PF zones CF7 (8.7 cm/1000 yr) and CF4 (0.6 cm/1000 yr), and lateral variation in sediment thickness suggest that the sediment deposition was strongly influenced by regional tectonic activity, including the uplift of the Gilf El Kebir Spur and subsidence of the Dakhla Basin.

4. Sediment deposition was predominantly cyclical, consisting of alternating shales and calcareous sandstones that are characterized by significant differences in clay mineralogies, geochemistry and fossil contents. In each cycle, the dark silty shales are generally barren of microfossils and represent deposition during sea-level highstands in restricted inner neritic to lagoonal environments characterized by euryhaline, dysaerobic or low oxygen conditions probably related to stagnating seas. The overlying fossiliferous calcareous sandstones reflect high-energy conditions during sea-level lowstand periods. The glauconitic silty shales overlying the sandstones represent periods of condensed sedimentation with influxes of terrestrial organic matter during maximum flooding, followed by deposition of dark muds (forming shales) during sea-level highstand periods.

5. Climatic conditions inferred from clay mineralogy and fossils indicate a tropical to subtropical environment characterized by seasonally humid conditions during the early to middle Maastrichtian. Perennially humid conditions prevailed during the latest Maastrichtian and early Paleocene with *Nypa* palm mangroves in tropical swamps, estuaries and tidal shores.

Acknowledgements

We gratefully acknowledge discussions with Jerry Baum and Karl Föllmi, as well as comments and suggestions by two anonymous reviewers. This publication was sponsored by the US-Egypt Science and Technology Joint Fund in cooperation with NSF and NRC under Project OTH2-008-001-98, NSF INT-9811030 (AT and GK), Deutsche Forschungsgemeinschaft DFG grant Sti 128/4-1 (WS) and the Swiss National Science Fund No. 8220-02837 (TA).

References

Abbas, H. L. & Habib, M. M. 1969. Stratigraphy of west Mawhoob area, Southwestern Desert, Egypt. *Institute Desert d'Egypt, Bulletin* **19** (2), 48–108.

Abdel-Kireem, M. R. & Samir, A. M. 1995. Biostratigraphic implications of the Maastrichtian–Lower Eocene sequence at the North Gunna section, Farafra Oasis, Western Desert, Egypt. *Marine Micropaleontology* **26**, 329–340.

Abdel-Kireem, M. R., Schrank, E., Samir, A. M. & Ibrahim, M. I. A. 1996. Cretaceous paleoecology, paleogeography and paleoclimatology of the North Western Desert, Egypt. *Journal of African Earth Sciences* **22**, 93–112.

Abdel Razik, T. M. 1969. Stratigraphical studies on the phosphate deposits between River Nile and Red Sea (south latitude 27°N). *Faculty of Science, Bulletin, Cairo University* **42**, 299–324.

Abdel Razik, T. M. 1972. Comparative studies on the Upper Cretaceous–Early Paleogene sediments on the Red Sea coast, Nile Valley and Western Desert, Egypt. *Sixth Arab Petroleum Congress, Algeria* **71**, 1–23.

Abramovich, S., Almogi, L. A. & Benjamini, C. 1998. Decline of the Maastrichtian pelagic ecosystem based on planktic Foraminifera assemblage change; implication for the terminal Cretaceous faunal crisis. *Geology* **26**, 63–66.

Adatte, T., Stinnesbeck, W. & Keller, G. 1996. Lithostratigraphic and mineralogic correlations of near K/T boundary clastic sediments in northeastern Mexico: implications for origin and nature of deposition. *Geological Society of America, Special Paper* **307**, 211–226.

Adatte, T., Keller, G. & Stinnesbeck, W. (in press). Late Cretaceous to early Paleocene climate and sea-level fluctuations. *Palaeogeography, Palaeoclimatology, Palaeoecology*.

Allam, A. M. 1986. A regional and paleoenvironmental study on the Upper Cretaceous deposits of the Bahariya Oasis, Libyan Desert, Egypt. *Journal of African Earth Sciences* **5**, 407–412.

Almogi-Labin, A., Flexer, A., Honigstein, A., Rosenfeld, A. & Rosenthal, E. 1990. Biostratigraphy and tectonically controlled sedimentation of the Maastrichtian in Israel and adjacent countries. *Revista Española de Paleontología* **5**, 41–52.

Anderson, L. D. & Delaney, M. L. 2000. Sequential extraction and analysis of phosphorus in marine sediments: streamlining of the SEDEX procedure. *Limnology and Oceanography* **45**, 509–515.

Awad, G. H. & Abed, M. 1969. Biostratigraphical zoning of the lower Tertiary in the Dakhla Oasis. *Geological Survey, UAR* **47**, 63 pp.

Awad, G. H. & Ghobrial, M. G. 1965. Zonal stratigraphy of the Kharga Oasis. *Ministry of Industry, General Egyptian Organisation for Geological Research and Mining, Geological Survey, Cairo* **34**, 77 pp.

Awad, G. H., Naim, E. M. & Abdou, H. F. 1964. The Campanian-Maastrichtian boundary and the Phosphate Series. *Faculty of Science, Bulletin, Alexandria University* **6**, 257–270.

Barrera, E., Savin, S. M., Thomas, E. & Jones, C. E. 1997. Evidence for thermohaline-circulation reversals controlled by sea-level change in the latest Cretaceous. *Geology* **25**, 715–718.

Barthel, W. K. & Herrmann-Degen, W. 1981. Late Cretaceous and early Tertiary stratigraphy in the Great Sand Sea and its SE margins (Farafra and Dakhla oases, SW Desert Egypt). *Mitteilungen der Bayerischen Staatssammlung für Paläontologie und Historische Geologie* **21**, 141–182.

Berggren, W. A., Kent, D. V., Swisher, C. C., III & Aubry, M.-P. 1995. A revised Cenozoic geochronology and chronostratigraphy. In *Geochronology, time scales and global stratigraphic correlation* (eds Berggren, W., Kent, D. V., Aubry, M.-P. & Hardenbol, J.), *Society for Sedimentary Geology, Special Publication* **54**, 129–212.

Bralower, T. J., Zachos, J. C., Thomas, E., Parrow, M., Paull, C. K., Kelley, D. C., Premoli Silva, I., Slier, W. V. & Lohmann, K. C. 1995. Late Paleocene to Eocene paleoceanography of the equatorial Pacific Ocean: stable isotopes recorded at Ocean Drilling Program Site 865, Allison Guyot. *Paleoceanography* **10**, 841–865.

Caron, M. 1985. Cretaceous planktic foraminifera. In *Plankton stratigraphy* (eds Bolli, H. M., Saunders, J. B. & Perch-Nielsen, K.), pp. 17–86 (Cambridge University Press, Cambridge).

Chamley, H. 1989. *Clay sedimentology*, 623 pp. (Springer-Verlag, Berlin).

Chamley, H., Deconinck, J. F. & Millot, G. 1990. Sur l'abondance des minéraux smectitiques dans les sédiments marins communs déposés lors des périodes de haut niveau marin du Jurassique au Paléogène. *Comptes Rendus de l'Académie des Sciences, Paris* **311** (II), 1529–1536.

Doeven, P. H. 1983. Cretaceous nannofossil stratigraphy and paleoecology of the Canadian Atlantic Margin. *Geological Survey of Canada, Bulletin* **356**, 1–70.

Dominik, W. 1985. *Stratigraphie und Sedimentologie (Geochemie, Schwermineralanalyse) der Oberkreide von Bahariya und ihre Korrelation zum Dakhla-Becken (Western Desert, Ägypten)*, 173 pp. (D. Reimer, Berlin).

El Akkad, S. & Dardir, A. A. 1966. Geology and phosphate deposits of Wasif–Safaga area. *Geological Survey of Egypt* **36**, 1–35.

El-Dawoody, A. S. & Zidan, M. A. 1976. Micro and nanno-paleontology of the Upper Cretaceous–Paleocene succession in west Mawhoob area, Dakhla Oasis, Egypt. *Revista Española de Micropaleontología* **8**, 401–428.

El Deftar, T., Issawi, B. & Abdallah, A. M. 1978. Contributions to the geology of Abu Tartur and adjacent areas: Western Desert Egypt. *Annals of the Geological Survey of Egypt* **8**, 51–90.

El Naggar, Z. R. 1966. Stratigraphy and planktonic foraminifera of the Upper Cretaceous–Lower Tertiary succession in the Esna-Idfu region, Nile Valley, Egypt, U.A.R. *British Museum (Natural History) Bulletin, Supplement* **2**, 279 pp.

Eshet, Y., Moshkovitz, S., Habib, D., Benjamini, C. & Magaritz, M. 1992. Calcareous nannofossil and dinoflagellate stratigraphy across the Cretaceous/Tertiary boundary at Hor Hahar, Israel. *Marine Micropaleontology* **18**, 199–228.

Faris, M. 1984. The Cretaceous-Tertiary boundary in central Egypt (Duwi region, Nile Valley, Kharga and Dakhla oases). *Neues Jahrbuch für Geologie und Paläontologie, Abhandlungen* **7**, 385–392.

Faris, M. & Strougo, A. 1998. The lower Libyan in Farafra (Western Desert) and Luxor (Nile Valley): correlation by calcareous nannofossils. *Middle East Research Center, Ain Shams University, Earth Science Series* **12**, 137–156.

Galal, G. M. I. 1995. *Paleoecology of microfossils and facies geology in the Paleogene of the northern part of El Quss Abu Said, Western Desert Egypt.* Unpublished PhD thesis, Alexandria University, 195pp.

Ganz, H. H., Luger, P., Schrank, E., Brooks, P. & Fowler, M. 1990a. Facial evolution of Late Cretaceous black shales from southeast Egypt. In *Research in Sudan, Somalia, Egypt and Kenya; results of the special research project 'Geoscientific problems in arid and semiarid areas'* (Sonderforshungsbereich 69); period 1987–1990 (eds Klitzsch, E. & Schrank, E.), *Berliner Geowissenschaftliche Abhandlungen Reihe A, Geologie und Paläontologie* **120** (2), 993–1010.

Ganz, H. H., Schrank, E., Brooks, P. W. & Fowler, M. G. 1990b. Facies evolution of Late Cretaceous black shales from southeast Egypt. In *Deposition of organic facies* (ed. Huc, Y.), *American Association of Petroleum Geologists, Bulletin* **30**, 229–217.

Garrison, R. F., Glenn, C. R., Snavely, P. D. & Mansour, S. E. A. 1979. Sedimentology and origin of Upper Cretaceous phosphorite deposits at Abu Tartur, Western Desert, Egypt. *Annals of the Geological Survey of Egypt* **9**, 261–281.

Glenn, R. C. 1990. Depositional sequences of the Duwi, Sibaiya and Phosphate formations, Egypt: phosphogenesis and glauconitization in a Late Cretaceous epeiric sea. In *Phosphorite research and development* (eds Notholt, A. J. G. & Jarvis, I.), *Geological Society, London, Special Publication* **52**, 205–222.

Gradstein, F. M., Agterberg, F. P., Ogg, J. G., Hardenbol, J., van Veen, P., Thierry, J. & Huang, Z. 1995. A Triassic, Jurassic and Cretaceous time scale. In *Geochronology, time scale and global stratigraphic correlation* (eds Berggren, W. A., Kent, D. V., Aubry, M. P. & Hardenbol, J.), *SEPM* (*Society of Sedimentary Geology*), *Special Publication* **54**, 95–128.

Hamama, H. H. & Kassab, A. S. 1990. Upper Cretaceous ammonites of Duwi Formation in Gabal Abu Had and Wadi Hamama, Eastern Desert, Egypt. *Journal of African Earth Sciences* **10**, 453–464.

Haq, B. U., Hardenbol, J. & Vail, P. R. 1987. Chronology of fluctuating sea-levels since the Triassic. *Science* **235**, 1156–1167.

Hassan, M. Y. 1973. Correlation of the Cretaceous-Tertiary contact in the oases of the Southwestern Desert of Egypt with that in the Djofra Graben, eastern Tripolitania, Libya. *Ain Shams Science Bulletin* **15**, 1–17.

Hendriks, F., Luger, P., Kallenbach, H. & Schroeder, J. H. 1984. Stratigraphical and sedimentological framework of the Kharga–Sinn el Kaddab Strech (western and southern part of the Upper Nile Basin), Western Desert Egypt. *Berliner Geowissenschaftliche Abhandlungen A* **50**, 117–151.

Hendriks, F., Luger, P., Biwitz, J. & Kallenbach, H. 1987. Evolution of the depositional environments of SE Egypt during the Cretaceous and lower Tertiary. *Berliner Geowissenschaftliche Abhandlungen A* **75**, 49–82.

Hermina, M. 1990. The surroundings of Kharga, Dakhla and Farafra oases. In *The geology of Egypt* (ed. Said, R.), pp. 259–292 (Balkema, Rotterdam/Brookfield).

Hermina, M. H., Ghobrial, M. G. & Issawi, B. 1961. *The geology of the Dakhla Oasis area*, 33 pp. (Geological Survey and Mineral Research Department, Cairo).

Hottinger, L. 1960. Recherches sur les Alvéolines du Paleocène et de l'Eocène. *Mémoire, Suisse Paléontologie* **75–76**, 234 pp.

Ibrahim, M. I. A. & Abdel-Kireem, M. R. 1997. Late Cretaceous palynofloras and foraminifera from Ain El-Wadi area, Farafra Oasis, Egypt. *Cretaceous Research* **18**, 633–660.

Issawi, B. 1972. Review of Upper Cretaceous–Lower Tertiary stratigraphy in central and southern Egypt. *American Association of Petroleum Geologists, Bulletin* **56**, 1448–1463.

Issawi, B., Hassan, M. Y. & Saad, E. N. 1978. Geology of the Abu Tartur Plateau, Western Desert, Egypt. *Annals of the Geological Survey, Egypt* **8**, 91–127.

Kassab, A., Kenawy, A. & Zakhira, M. 1995. Biostratigraphy of some Upper Cretaceous–lower Tertiary outcrops from the Egyptian Western Desert. *Neues Jahrbuch für Geologie und Paläontologie, Abhandlungen* **196**, 309–326.

Kassab, A. S. & Zakhira, M. S. 1995. Maastrichtian and Paleocene bivalves from the Western Desert, Egypt. *Neues Jahrbuch für Geologie und Paläontologie, Abhandlungen* **196**, 327–346.

Keller, G., Adatte, T., Stinnesbeck, W., Stuben, D., Kramar, U., Berner, Z., Li, L. & Perch-Nielsen, K. 1998. The Cretaceous-Tertiary transition in the shallow Saharan platform of southern Tunisa. *Geobios* **30**, 951–975.

Keller, G., Li, L. & MacLeod, N. 1995. The Cretaceous/Tertiary boundary stratotype section at El Kef, Tunisia: How catastrophic was the mass extinction? *Paleogeography, Paleoclimatololgy, Paleoecology* **119**, 221–254.

Keller, G. & Stinnesbeck, W. 1996. Sea level changes, clastic deposits, and megatsunamis across the Cretaceous-Tertiary boundary. In *The Cretaceous/Tertiary boundary mass extinction: biotic and environmental changes* (eds MacLeod, N. & Keller, G.), pp. 415–450 (W. W. Norton & Co., New York).

Kennedy, W. J., Cobban, W. A. & Scott, G. R. 1992. Ammonite correlation of the uppermost Campanian of Western Europe, the U. S. Gulf Coast, Atlantic Seaboard and Western Interior, and the numerical age of the base of the Maastrichtian. *Geological Magazine* **129**, 497–500.

Klitzsch, E. 1986. Plate tectonic and cratonal geology in northeast Africa (Egypt/Sudan). *Geologische Rundschau* **75**, 755–768.

Klitzsch, E. & Wycisk, P. 1987. Geology of the sedimentary basins of northern Sudan and bordering areas. *Berliner Geowissenschaftliche Abhandlungen A* **75**, 47–79.

Kübler, B. 1983. Dosage quantitatif des minéraux majeurs des roches sédimentaires par diffraction X. *Cahier de l'Institut de Géologie de Neuchâtel, Série ADX* **1**, 12 pp.

Kübler, B. 1987. Cristallinite de l'illite, methods normaisees de preparations, methods normalisees de measures. *Cahiers Institut de Géologie, Neuchâtel, Suisse, Série ADX* **1**.

Li, L. & Keller, G. 1998a. Maastrichtian climate, productivity and faunal turnovers in planktic foraminifera in South Atlantic DSDP sites 525 and 21. *Marine Micropaleontology* **33**, 55–86.

Li, L. & Keller, G. 1998b. Maastrichtian diversification of planktic foraminifera at El Kef and Elles, Tunisia. *Eclogae Geologicae Helvetiae* **91**, 75–102.

Li, L., Keller, G. & Stinnesbeck, W. 1999. The Late Campanian and Maastrichtian in northwestern Tunisia: paleoenvironmental inferences from lithology, macrofauna and benthic foraminifera. *Cretaceous Research* **20**, 231–252.

Li, L., Keller, G., Adatte, T. & Stinnesbeck, W. 2000. Late Cretaceous sea-level changes in Tunisia: a multi-disciplinary approach. *Journal of the Geological Society, London* **157**, 447–458.

Luger, P. 1988. Maastrichtian to Paleocene facies evolution and Cretaceous/Tertiary boundary in middle and southern Egypt. *Revista Española de Micropaleontologia, Numero Extraordinario* 83–90.

Luger, P. & Schrank, E. 1987. Mesozoic to Paleogene transitions in middle and southern Egypt – summary of paleontological evidence. In *Current Research in African Earth Sciences* (eds Matheis, G. & Schandelmeir, H.) pp. 199–202 (Balkema, Rotterdam).

MacLeod, N. & Keller, G. 1991. How complete are Cretaceous/Tertiary boundary sections? A chronostratigraphic estimate based on graphic correlation. *Geological Society of America, Bulletin* **103**, 1439–1457.

Mansour, H. H., Issawi, B. & Askalany, M. M. 1982. Contribution to the geology of West Dakhla oasis area, Western Desert, Egypt. *Annals of the Geological Survey of Egypt* **12**, 255–281.

Martini, E. 1971. Standard Tertiary and Quaternary calcareous nannoplankton zonation. *Proceedings of the Second Planktonic Conference* (Roma, 1970), 739–785.

Nederbragt, A. J. 1991. Late Cretaceous biostratigraphy and development of Heterohelicidae (planktic foraminifera). *Micropaleontology* **37**, 329–372.

Obradovich, J. D. 1993. A Cretaceous time scale. In *Evolution of the Western Interior Basin* (eds Caldwell, W. G. & Kaufman, E. G.), *Geological Association of Canada, Special Paper* **39**, 379–396.

Odin, G. S. 1996. Definition of a Global Boundary Stratotype Section and Point for the Campanian/Maastrichtian boundary. *Bulletin de l'Institute Royal des Sciences Naturelles de Belgique, Sciences de Terre* **66** (Supplement), 111–117.

Okada, H. & Bukry, D. 1980. Supplementary modification and introduction of code numbers to the low-latitude coccolith biostratigraphic zonation (Bukry, 1973, 1975). *Marine Micropaleontology* **5**, 321–325.

Omara, S., Philobbos, E. R. & Mansour, H. H. 1976. Contribution to the geology of the Dakhla Oasis area, Western Desert, Egypt. *Bulletin of the Faculty of Science, Assiut University* **5**, 319–339.

Omara, S., Philobbos, E. R. & Mansour, H. H. 1977. Contribution to the geology of the phosphorites of the Dakhla Oasis area, Western Desert, Egypt. *First Conference on Mining and Metallurgical Technology, Assiut University*, pp. 21–35.

Pardo, A., Ortiz, N. & Keller, G. 1996. Latest Maastrichtian and K/T boundary foraminiferal turnover and environmental changes at Agost, Spain. In *The Cretaceous-Tertiary boundary mass-extinction: biotic and environmental events* (eds MacLeod, N. & Keller, G.), pp. 155–176 (W. W. Norton & Co., New York).

Perch-Nielsen, K. 1979. Calcareous nannofossil Cretaceous/Tertiary boundary sections in Denmark. In *Cretaceous/Tertiary boundary event-symposium* (Copenhagen) **1** (eds Birklund, T. & Bromley, R. G.), pp. 120–126.

Perch-Nielsen, K. 1981a. New Maastrichtian and Paleocene calcareous nannofossils from Africa, Denmark, the USA and the Atlantic, and some Paleocene lineages. *Eclogae Geologicae Helvetiae* **73**, 831–863.

Perch-Nielsen, K. 1981b. Les nannofossiles calcaires à la limite Crétacé-Tertiaire prés de El Kef, Tunisie. *Cahiers de Micropaleontologie* **3**, 25–37.

Perch-Nielsen, K. 1983. Recognition of Cretaceous stage boundaries by means of calcareous nannofossils. In *Abstracts, Symposium on Cretaceous Stage boundaries* (Copenhagen) (ed. Brikelund, T.), pp. 152–156.

Perch-Nielsen, K. 1985. Cenozoic calcareous nannofossils. In *Plankton stratigraphy* (Bolli, H. M., Saunders, J. B. & Perch-Nielsen, K.), pp. 422–454 (Cambridge University Press, Cambridge).

Reiss, Z. 1962. Stratigraphy of phosphate deposits in Israel. *Geological Survey of Israel, Bulletin* **4**, 1–23.

Reiss, Z. 1984. Stratigraphy of phosphate deposits in Israel. *Geological Survey of Israel, Bulletin* **34**, 1–23.

Reiss, Z., Almogi-Labin, A., Honigstein, A., Lewy, Z., Lipson-Benitah, S., Moshkovitz, S. & Zaks, Y. 1985. Late Cretaceous multiple stratigraphic framework of Israel. *Israel Journal of Earth Sciences* **34**, 147–166.

Robaszynski, F., Caron, M., Gonzalez Donoso, J. M., Wonders, A. A. H. & The European Working Group on Planktonic Foraminifera, 1983–1984. Atlas of Late Cretaceous globotruncanids. *Revista Española de Micropaleontología* **26**, 145–305.

Romein, W. M. 1979. Lineages in early Paleocene nannoplankton. *Utrecht Micropaleontological Bulletin* **22**, 18–22.

Roth, P. H. 1978. Cretaceous nannoplankton biostratigraphy and paleoceanography of the northwestern Atlantic Ocean. *Initial Reports of the Deep Sea Drilling Project* **44**, 731–759.

Ruttenberg, K. C. 1992. Development of a sequential extraction method for different forms of phosphorus in marine sediments. *Limnology and Oceanography* **37**, 1460–1482.

Ruttenberg, K. C. & Berner, R. A. 1993. Authigenic apatite formation and burial in sediments from non-upwelling, continental margin environments. *Geochimica et Cosmochimica Acta* **57**, 991–1007.

Said, R. 1961. Tectonic framework of Egypt and its influence on distribution of foraminifera. *American Association of Petroleum Geologists, Bulletin* **45**, 198–218.

Said, R. 1962. *The geology of Egypt*, 377 pp. (Elsevier, Amsterdam).

Said, R. & Kerdany, M. T. 1961. The geology and micropaleontology of the Farafra Oasis, Egypt. *Micropaleontology* **7**, 317–336.

Samir, A. M. 1994. Biostratigraphy and paleoecology of the Khoman Formation (Upper Cretaceous) between the Bahariya and the Farafra oases, Western Desert, Egypt. *Neues Jahrbuch für Geologie and Paläontologie, Abhandlungen* **191**, 271–297.

Samir, A. M. 1995. Paleoenvironmental significance of the Upper Cretaceous–Lower Tertiary foraminifera of the North Gunna section, Farafra Oasis, Western Desert, Egypt. *Proceedings, Koninklijke Nederlandsch Akademie van Wetenschappen* **98**, 109–126.

Schrank, E. 1984. Organic-walled microfossils and sedimentary facies in Abu Tartur phosphates (Late Cretaceous, Egypt). *Berliner Geowissenschaftliche Abhandlungen A* **50**, 177–187.

Schrank, E. 1987. Paleozoic and Mesozoic palynomorphs from northeast Africa (Egypt and Sudan) with special references to Late Cretaceous pollen and dinoflagellates. *Berliner Geowissenschaftliche Abhandlungen A* **75.1**, 249–310.

Schrank, E. & Perch-Nielsen, K. 1985. Late Cretaceous palynostratigraphy in Egypt with comments on Maastrichtian and Early Tertiary calcareous nannofossils. *Newsletters on Stratigraphy* **15**, 81–99.

Sissingh, W. 1977. Biostratigraphy of Cretaceous calcareous nannoplankton. *Geologie en Mijnbouw* **56**, 37–65.

Slaughter, B. H. & Thurmond, J. T. 1974. A Lower Cenomanian 'Cretaceous' ichthyofauna from the Bahariya Formation of Egypt. *Annals of the Geological Survey of Egypt* **4**, 25–40.

Smith, J. B., Lamanna, M. C., Lacovara, K. J., Dodson, P., Smith, J. R., Poole, J. C., Giegengack, R. & Attia, Y. 2001. A giant sauropod dinosaur from an Upper Cretaceous mangrove deposit in Egypt. *Science* **292**, 1704–1706.

Tantawy, A. A. 1998. *Stratigraphical and paleontological studies on some Paleocene–Eocene successions in Egypt*. Unpublished PhD thesis, Aswan Faculty of Science, South Valley University, Egypt, 273 pp.

Weaver, C. E. 1989. *Clays, muds and shales*, 819 pp. (Developments in Sedimentology, 44, Elsevier, Amsterdam).

Werner, C. 1989. Die Elasmobranchier-Fauna des Gebel Dist Member der Bahariya Formation (Obercenoman) der Oase Bahariya, Ägypten. *PalaeoIchthyologica* **5**, 1–112.

Youssef, M. & Abdel-Aziz, W. 1971. Biostratigraphy of the Upper Cretaceous–Lower Tertiary in Farafra Oasis, Libyan Desert, Egypt. In *Symposium on the geology of Libya* (ed. Gray, L. G.), pp. 227–249 (Faculty of Science, University of Libya, Benghazi).